DOI: 10.24996/ijs.2022.63.7.27

ISSN: 0067-2904

Reservoir Characterization of Lower Qamchuqa (Shu'aiba) Formation from the Well BH-86, Bai- Hassan Oil field, Northern Iraq

Sabir S. Shahab*[1], Dler H. Baban[2], Lafta S. Kadhim[2]
[1]*Department of Applied Geology, College of Science, Tikrit University, Iraq*
[2]*Department of Geology, College of Science, Sulaimani University, Iraq*

Received: 26/4/2021 Accepted: 11/2/2022 Published: 30/7/2022

Abstract
The reservoir characterization of Lower Qamchuqa (Shu'aiba) Formation (Aptian) is studied at the well BH-86 of Bai- Hassan Oilfield in Kirkuk area, Northern Iraq. The lithological study (of 91 thin sections) revealed that the formation consists of shaly limestone, a thin bed of marl within the limestone, and dolomitic limestone. Four petrographic microfacies were noticed Lime mudstone microfacies, Dolomudstone microfacies, Lime wackestone microfacies, subdivided into benthonic foraminifera lime wackestone submicrofacies and bioclasts lime wackestone submicrofacies, and the last microfacies is the Lime packstone microfacies, which is subdivided into pelloidal lime packstone submicrofacies and Orbitolina lime packstone microfacies. Shale content is calculated from the gamma-ry log, showing that the formation is mainly of low shale content (less than 35%). The porosity determined from sonic, density, and neutron logs reflect that the range between <1 and 15% and in some intervals about 6% is secondary porosity type. The estimated permeability ranges between <0.01 and 2.0mD, reflecting low permeability. The formation is subdivided into six reservoir units according to the shale content, average porosity, and permeability. The unit RU-5 has the best reservoir properties among the identified units with an average shale content of about 3.15%, about 6.2% porosity, and about 1.75mD average permeability. On the other hand, the least reservoir property is noticed in the unit RU-1 with average 9.48% shale content, 3.64% porosity, and 0.5mD average permeability. The research indicates that the fractures contribute to the flow within the Lower Qamchuqa Formation. Fluids flow through the formation in four unique Hydraulic Flow Units (HFU). Only about 8% of the gross 146m of the formation is expected to have the required reservoir properties for oil production and about 68% for gas production. The actual productive thickness for oil is only about 2.8% of the gross thickness of the studied section, and it’s more than 50% of the gross thickness for gas.
Key Words: Shu’aiba Formation, Bai-Hassan oil field, Microfacies, Reservoir characterization, Net to Gross pay.

الخواص المكمنية لتكوين القمجوقة السفلي (الشعيبة) ذو العمر الأبتيان في البئر BH-86 من حقل باي حسن النفطي , شمال العراق

صابر صبحي شهاب[1*] , دلير حسين بابان[2], لفتة سلمان كاظم[2]
[1] قسم الجيولوجي, كلية العلوم, جامعة تكريت, العراق
[2] قسم الجيولوجي, كلية العلوم, جامعة السليمانية, العراق

*Email: sabir.s.shahab.geo301@st.tu.edu.iq

الخلاصه

تضمنت الدراسة الحالية تكوين قمجوقة السفلي (الشعيبة) بعمر الأبتيان حيث تم دراسة الخصائص المكمنية للتكوين في البئر المختار(BH–86) في حقل باي حسن في محافظة كركوك – شمالي العراق والذي يقع في نطاق الطيات الواطئة ضمن الرصيف غير المستقر.

من خلال دراسة 91 شريحة صخرية تبين بان التكوين يتالف من الحجر الجيري السجيلي وطبقة رقيقة من الطفل مع الحجر جيري, والحجر الجيري الدولومايتي.

اظهرت نتائج البتروغرافية للتكوين صخارية متباينة ومن خلالها اكتشف اربعة انواع من سحنات دقيقة رئيسية متمثلة بسحنة الحجر الجيري الطيني الرئيسية ، وسحنة الحجر الدولومايتي الرئيسية وسحنة الحجر الجيري الواكي الرئيسية والتي بدورها قسمت الى سحنتين ثانويتين هما سحنة الحجر الجيري الواكي الحامل للفورامنيفيرا القاعية و سحنة الحجر الجيري الواكي الحامل للفتات الحياتي, وأخيرا سحنة الحجر الجيري المرصوص الرئيسية والتي قسمت أيضا الى سحنتين ثانويتين هما سحنة الحجر الجيري المرصوص الحامل للدمالق و الحجر الجيري المرصوص الحامل للأوربيتولينا.

بينت الدراسة الحالية بان معظم أجزاء التكوين قيد الدراسة تحتوي على حجم سجيل بنسبة اقل من 35% واظهرت كل من المجسات الصوتية، الكثافة، والنيترون بان معدل المسامية محددة في التكوين ما بين اقل من1 % –15%. اظهرت تحاليل اللباب والمجسات باستخدام طريقة تحليل الانحدار المتعدد بان التكوين حاوية على نفاذية واطئة والتي تتراوح بين 0.01 الى 2 ملي دارسي. وقد وجد بان الجزء االعلوي من التكوين يحتوي على اعلى نسبة من المسامية الثانوية بلغت حولي 8 % اما الجزء الأوسط والأسفل من التكوين فقد اظهرا اقل من 3% من المسامية الثانوية.

تم تقسيم تكوين القمجوقة السفلى الى ستة وحدات مكمنية بالأعتماد على تباين حجم السجيل و معدل المسامية و النفاذية. اعتبرت الوحدة المكمنية RU– 5 افضل خصائص المكمنية من بين الوحدات المكمنية الاخرى بمعدل محتوى السجيلي % 3.15, مسامية 6.2%, و معدل نفاذية بلغت 1.75 ملي دارسي. كما واعتبرت الوحدة المكمنية RU –1 ذي الأقل من الصفات المكمنية بمعدل 9.48 % محتوى السجيلي, 3.64. % المسامية و 0.5 ملي دارسي كمعدل للنفاذية.

كما أظهرت الدراسة الحالية بان حركة الموائع في التكوين معتمدة بصورة كبيرة على وجود التكسرات و ان الموائع تجري في التكوين ضمن اربعة وحدات جريان هايدروليكية HFU .

لقد أستنتجت من الدراسة بأن 8% فقط من السمك الكلي للتكوين و البالغ 146م في البئر BH– 86 يحتوي على صفات مكمنية تؤهله لأنتاج النفط, بينما 68% من السمك الكلي للتكوين يحتوي على صفات مكمنية مناسبة لأنتاج الغاز. و قد تم أحتساب نسبة السمك الصافي الفعلي المنتج للنفط في البئر قيد الدراسة و كانت 2.8 % من السمك الكلي بينما بلغت النسبة اكثر من 50% بالنسبة للغاز.

1. Introduction

Iraq is considered one of the richest oil countries in the Middle East. The Cretaceous age sequences are considered to be as prolific as a reservoir in Iraq [1]. According to Al-Sakini, 1992 [2], Cretaceous successions include a lot of productive reservoirs and contain about 80% of Iraq's oil reserve and the Lower Cretaceous reservoir contains about 30% of the country's hydrocarbon reserves.

The Shu'aiba Formation (Lower Qamchuqa Formation) as a Cretaceous reservoir, is important in the process of petroleum exploration in Iraq. The discovered oil accumulated in this reservoir is documented in most of the Arabian Gulf's countries such as Oman, UAE, Qatar, and Kuwait [3] [4] [5]. In Saudi Arabia, Shu’aiba Formation is reported as a source of generating oil in addition to its action as a potential reservoir [6] [7].

Many researchers have investigated the Lower Qamchuqa Formation in Iraq [1] [8] [9] [10] [11] [12] [13] [14]. The Lower Qamchuqa (Shu’aiba) Formation in Bai-Hassan Oilfield comprises of three units: the upper and middle units consist of limestone dominant lithology, while the lower unit (which represents the major part of the formation) consists of shaley limestone, limestone, and dolomite [15].

Al-Shdidi, et al., 1995 [16] mentioned that Middle Sarmord Formation and Lower Qamchuqa Formation are belonging to the MS I megasequence which corresponds to a regressive megasequence. They further subdivided the MS I to two mesosequences namely S1 and S2. The S2, which represented Lower Qamchuqa Formation, appeared to be composed entirely of carbonates and showed a regressive evolution and development of neritic dolomitic limestone.

Al-Eisa,1997 [17] concluded that the depositional environment of the Shu'aiba Formation is *Orbitolina* shoal environment.

Ameen, 2007 [18] mentioned that the formation deposited in a low-energy environment represents reef, backreef, forereef and lagoonal environments.

Sadeq, et al., 2015 [19] used a new method to estimate the secondary porosity and absolute permeability of the fractured and vuggy carbonate formations in Bai-Hassan Oilfield. They concluded that the formation exhibits a triple porosity petrophysical system which shows intercrystalline, intracrystalline, moldic, vuggy and fractured porosity types. They also mentioned that the average fracture porosity in the formation is about 0.07, with average permeability of 1.6 mD.

Qader and Al-Qayim, 2016, [20], subdivided the Lower Qamchuqa in Khabbaz Oilfield into three lithological units: the upper 8-15 m (unit A) is consists of partly dolomitized marly limestones, while the middle 52m to 56m (unit B) is consists of vuggy dolomitic limestone and dolostone, whereas the lower than110m (C unit) is consists of shale-rich and dolomitic limestones. They are also mentioned that the Limestone microfacies include shelfal bioclastic wackestones, *Orbitolina* bioclastic packstones, *Orbitolina* grainstones, and pelagic bioclastic wackestones.

This study is an attempt to show the reservoir property of the Lower Qamchuqa (Shu'aiba) Formation within Bai- Hassan Oilfield, Northern Iraq, using the available rock and log data.

1.1 Geologic and Tectonic Settings

The Qamchuqa sequence studied in its type section was represented by massive, rather argillaceous, fossiliferous limestones, with some disseminated quartz silt, sometimes glauconitic, usually dolomitized, interbedded with crystalline dolomites [1]. Whereas the Shu'aiba Formation which is included into the Lower Qamchuqa Formation in its sub-surface type area (Zubair structure, well No.3) comprised of argillaceous, chalky, and crystalline limestones, with some pseudo-oolitic limestones, glauconitic in parts [10].

The Lower Qamchuqa (Shu'aiba) Formation sediments are acquired a distinct importance due to being one of the Cretaceous reservoirs in a number of the Iraqi oilfields [10] and [14].

The Lower Qamchuqa Formation's thickness in the High Folded Zone is extremely variable ranging between 250m and 300m and reaching up to 500m [1]. Whereas it has different thicknesses in the sub-surface sections ranging from 19m in the well K-77 in the Kirkuk structure to 421m in the well Abu-Khaima-1 [11].

The Lower Qamchuqa (Shu'aiba) Formation was deposited in a purely marine neritic environment which affected slightly by terrigenous supply [1]. The formation is representing shallow microfacies (Neritic to Shoal Facies) [21] and [22].

The formation in the Bai-Hassan Oilfield (the study area) is overlained unconformably by the shale beds of Nahr Umr Formation and underlained conformably by Garagu Formation [15].

The age of the Lower Qamchuqa Formation is considered as Early-Aptian depending on some index fossils such as *Orbitolina lenticularis* [23]. The common index fossils that indicating the formation age were represented by *Choffatella decipiens* and *Orbitolina* cf *lenticularis* with *Acicularia* cf. and others which firmly established the formation age as Hauterivian till Aptian [1].

The study area, Bai-Hassan Oilfield, is situated in Northern Iraq within the Zagros Fold Belt or within the Low Folded Zone of the unstable shelf of the physiographic divisions of Iraq (Fig. 1A) [25].

Bai-Hassan Oilfield is located in Kirkuk Governorate and structurally consists of a double plunging asymmetrical longitudinal anticline of about 32km length and about 3km width and extends parallel to the Kirkuk structure at its southwestern side. The axis of the structure is sinuous in shape and has a Northwest-Southeast trend (Fig. 1B). The structure of Bai-Hassan consists of two domes; Kithka at the south and Dawood at the north (being Kithka bigger and higher than the Dawood) and both domes are separated by a Shahl saddle. The first exploration well drilled in the field was in 1929 [24], and currently, the field produces from two main reservoirs known as Tertiary and Cretaceous reservoirs [15].

The depositional basin in Iraq has undergone an open phase toward NNE-SSW in the Upper Triassic – Early Upper Cretaceous and formed sedimentary basins in which most of the Cretaceous sediments accumulated on the north edge of the Arabian Plate [15].

Since the Early Upper Cretaceous, the sedimentary basin has started converging due to the collision of both the Arabian and Eurasian Plate. With appearing the Zagros Main Fault and continuing convergence till the Late Paleocene another phase of compressional movement occurred which lead to form the Low Folded Zone in Iraq including the structure of the Bi-Hassan Oilfield (Fig. 1A) [15].

2. Data and Methodology

The selected well is BH-86 within Bai- Hassan Oilfield, which is located at the northern Dawood Dome (Fig. 1B). Lower Qamchuqa Formation in this well appears between depths 2174m and the total depth of the well at 2321m with a drilled thickness of about 146m. The Albian Nah Umr Formation overlays the studied Lower Qamchuqa Formation in the selected well.

The used data in this study include:

1. Twenty-one rock samples from the Lower Qamchuqa Formation from which 21 thin sections are prepared.
2. The available 70 thin sections prepared by the Northern Oil Company (NOC) in Kirkuk for the Lower Qamchuqa Formation in the studied well [15].
3. The conventional log data of Caliper, Gamma ray, Spontaneous Potential, Sonic, Density, Neutron, and Resistivity logs are collected from the Northern Oil Company (NOC) in Kirkuk [15] as well.
4. Porosity and permeability values are calculated and measured from core test analysis done for selected intervals from the formation in the studied well.

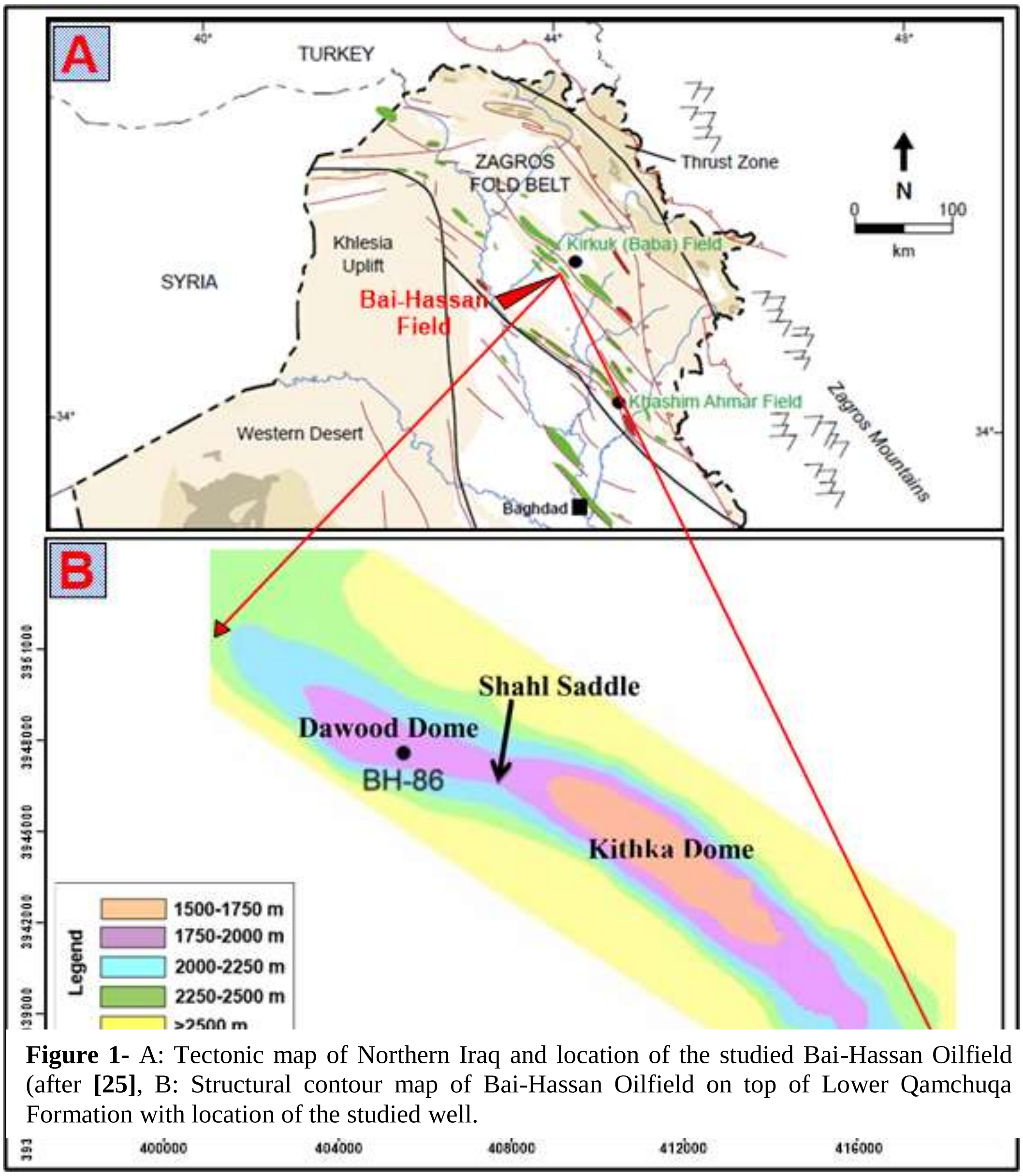

Figure 1- A: Tectonic map of Northern Iraq and location of the studied Bai-Hassan Oilfield (after **[25]**, B: Structural contour map of Bai-Hassan Oilfield on top of Lower Qamchuqa Formation with location of the studied well.

All the information about the depths of the studied thin sections that prepared by the authors and by NOC respectively for selected rock samples from Lower Qamchuqa Formation in the studied well are tabulated in Tables 1&2 [15].

Table 1- Depths of the studied thin sections prepared by the authors for Lower Qamchuqa Formation from the well BH-86

Sample No.	Depth (m)	Sampl e No.	Depth (m)	Sampl e No.	Depth (m)	Sampl e No.	Depth (m)	Sampl e No.	Depth (m)
1	2174	**6**	2207	**11**	2245	**16**	2285	**21**	2320
2	2175	**7**	2216	**12**	2250	**17**	2290	**-**	-
3	2180	**8**	2225	**13**	2260	**18**	2300	**-**	-
4	2190	**9**	2230	**14**	2270	**19**	2305	**-**	-
5	2200	**10**	2237	**15**	2280	**20**	2310	**-**	-

Table 2- Depths of the studied thin sections prepared by NOC for Lower Qamchuqa Formation from the well BH-86

Samp. No.	Depth (m)	Samp. No.	Depth (m)	Samp. No.	Depth (m)	Samp. No.	Depth (m)
1	2174	**19**	2206-2206.8	**37**	2223.20	**55**	2269-2270
2	2175	**20**	2206.8-2207.6	**38**	2224	**56**	2270-2284
3	2176	**21**	2208.45	**39**	2224.85	**57**	2284-2288
4	2177-2178	**22**	2209.25	**40**	2225.65	**58**	2291-2292
5	2180-2181	**23**	2210.15	**41**	2226.5	**59**	2293-2294
6	2184	**24**	2211	**42**	2227.25	**60**	2295-2296
7	2186	**25**	2211.75	**43**	2228.10	**61**	2297-2298
8	2189	**26**	2212.6-2213.4	**44**	2228.90	**62**	2299-2300
9	2190	**27**	2213.40-2214.2	**45**	2229.7	**63**	2301-2302
10	2192	**28**	2214.20-2215	**46**	2230.55	**64**	2303-2304
11	2193	**29**	2215.8	**47**	2231.40	**65**	2305-2306
12	2194	**30**	2215.8-2216.5	**48**	2232.20	**66**	2309-2310
13	2201	**31**	2216.5-2217.40	**49**	2233	**67**	2311-2312
14	2202	**32**	2217.4-2218.25	**50**	2233-2242	**68**	2315-2316
15	2203	**33**	2219.95	**51**	2242-2246	**69**	2317-2318
16	2204	**34**	2220.75	**52**	2260-2261	**70**	2319-2320
17	2205	**35**	2221.55	**53**	2263-2264	-	-
18	2206	**36**	2222.35	**54**	2267-2268	-	-

The following procedures of preparing the samples are applied:
1. Preparing 21thin sections (Table-1) and examining them with the rest 70 thin sections from the NOC (Table-2) using polarized microscopy to determine the important sedimentological and petrographical properties of the formation.
2. Analyzing selected 20 samples (core & cutting) by Calcimetry instrument to determine the ratios of the calcite, dolomite, and residual materials.
3. Digitizing the available logs using Neural software.
4. Calculating the reservoir parameters and re-plotting the digitized curves using Excel software.
5. Drawing stratigraphic columns, correlation sections, maps, collective curves, and the crossplots using Log Plot, Surfer, GIS, Grapher, and Petrel software.

3. Results and Discussion

a. Lithological Description

The analysis of selected 20 samples (core & cutting) by applying the Calcimetry instrument to determine the percentages of the calcite, dolomite, and residual materials, reflect that the average percentage of the total carbonate rock is 72.65% composed of 61.55% calcite and 11.1 % dolomite while the rest is the insoluble residue that represent 23.85 % as average (Table-3).

The existed record of the gamma ray log with the calcimetry analysis that done for a number of selected rock samples supported the process of lithology determination (Figure 2). The lithologic description of the Lower Qamchuqa Formation in the studied well is shown in Table.4.

Table 3- Concentration of Calcite (CaCO3), Dolomite (CaMg (CO3)2) and Insoluble Residue in the Lower Qamchuqa Formation of the studied samples.

BH-86 Interval Depth-m	Calcite $CaCo_3$ %	Dolomite $Mg(CaCo_3)_2$ %	Total Carbonate %	Insoluble Residue %
2174	48	3	51	49
2175	62	4	66	34
2180	41	5	46	54
2190	51	4	55	45
2200	61	9	70	30
2207	10	14	24	6
2216	75	17	92	8
2225	64	17	81	19
2230	87	34	121	4
2237	55	9	64	11
2245	52	20	72	28
2250	78	5	83	17
2260	70	11	81	19
2270	61	6	67	33
2280	49	5	54	32
2285	53	19	72	42
2300	82	5	87	13
2305	73	13	86	14
2310	79	10	89	11
2320	80	12	92	8
Avg.	61.55	11.1	72.65	23.85

Contamination intervals

Table 4- Lithology description of the Lower Qamchuqa Formation in the studied BH-86 well.

Formation	Depth Intervals m		Lithology Descriptions
Lower Qamchuqa	2174-2222	Upper Part	Dark to light grey colored shaley limestone at (2174-2200) m. The data of the gamma ray showed relatively high shale content from depth (2200-2201) m and this approved through observing 30% insoluble residue by the calcimetry analysis.
			The lithology of the formation become olive grey limestone at depth interval 2201-2212m, then dense olive grey dolomitic limestone between depths 2212m and 2222m.
	2222-2265	Middle Part	At depths 2222-2231m, appeared light olive grey dolomite and become olive grey limestone at depth (2231-2237)m. Dark to light grey color shaley limestone at (2237-2240) m, and olive grey dolomitic limestone at depth (2240-2245) m. Dark to light grey shaley limestone appeared at (2245-2265) m with interbedded sections of olive grey limestone, and dolomite crystals with anhydrite in parts detected.
	2265-2321	Lower Part	Olive grey limestone, olive grey dolomitic limestone, and dark to light shaley limestone were observed at (2265-2280, 2280-2286, 2286-2295) m respectively with interbedded of thin bed of marl as approved by the gamma ray and results of the calcimetry analysis. The rest part of the formation was composed of successions of olive grey limestone (2295-2310) m with interbedded of thin dolomitic limestone beds, dark to light grey shaley limestone (2130-2317) m, and dolomitic limestone (2317-2321) m (Fig.2), (Table.3).

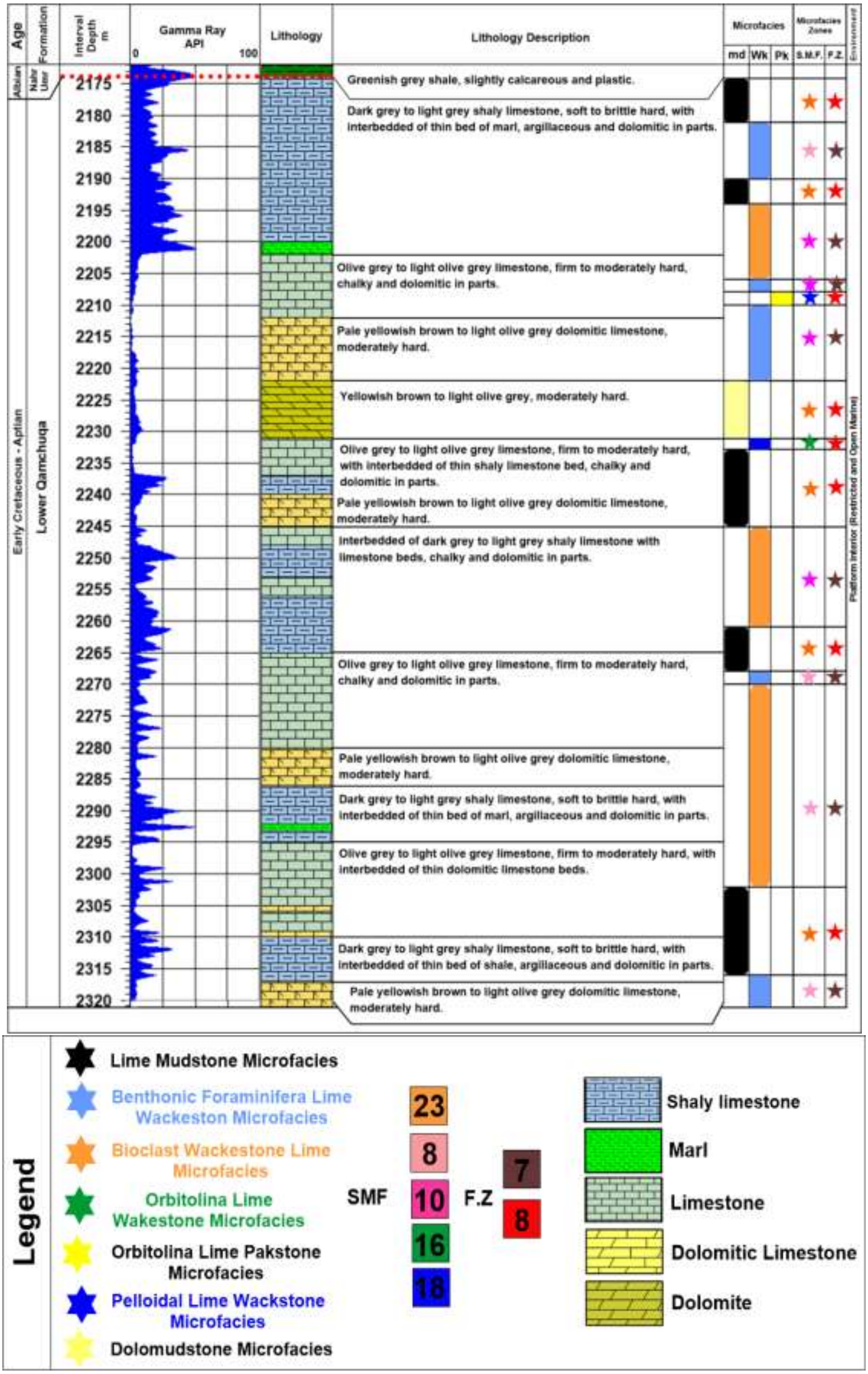

Figure 2- Stratigraphic column and Microfacies of the Lower Qamchuqa Formation in the well BH-86.

b. Microfacies

Four major types of microfacies with four sub-microfacies have been identified through optical study of the thin sections using polarized microscopy and depending on Dunham, 1962 classification [26]. In

Lime mudstone microfacies, Dolomudstone microfacies, and Lime wackestone microfacies are appeared to be the dominant microfacies types within the studied Lower Qamchuqa Formation. Packstone microfacies is noticed only in 2m thick interval between depths 2507m and 2509m, whereas no Grainstone type microfacies are recognized within the studied thin sections.

The Lower Qamchuqa Formation in the studied well looks to be deposited in an open marine environment fluctuated in to a restricted environment (platform interior environment).According to Flugel, 2004, the recognized components of the microfacies are represented as SMF and FZ [27].

The distribution of the different microfacies along the formation with their representative Standard Microfacies (SMF) and Facies Zones (FZ) of Flugel, 2004, a method [27] are shown in Figure 2.

c. Shale Volume

The Shale volume contents are calculated through the data of the gamma-ray log (Figure 3). Almost no higher than 60 °API gamma-ray was recorded along with the formation. Accordingly, no higher than 50% of shale volume content was noticed in the formation. Moreover, Ghorab, et al., 2008 method [28], is applied for distinguishing between the intervals based on the shale volume content. The upper part of the formation (between depths of 2174m and 2204m) appeared to be relative of the highest shale content (Table 5). Actually, the Gamma-ray log and the calculated shale content for the Lower Qamchuqa Formation in the well BH-86 indicated that a lot of clean intervals (<10% shale content) have existed as well as intercalated shaley intervals (between 10 and 35% shale content). Only few relatively narrow shale zones have been recognized along the section in which more than 35% shale content calculated (Figure 3).

Table 5- Shale content zonation and average volume of shale for Lower Qamchuqa Formation and for the lower most part of Nahr Umr Formation [28].

Well	Formation	Depth Interval (m)	Zonation	Thickness (m)	Avg. Vsh %
BH-86	Nahr Umr	2172-2174	Shaly zone	2	31.67
	Lower Qamchuqa	2174-2202	Shaly zone	28	24.05
		2202-2237	Clean zone	35	3.63
		2237-2240	Shaly zone	3	18.92
		2240-2248	Clean zone	8	6.07
		2248-2269	Shaly zone	21	15.91
		2269-2288	Clean zone	19	8.09
		2288-2295	Shaly zone	7	19.65
		2295-2299	Clean zone	4	4.03
		2299-2302	Shaly zone	3	14.75
		2302-2309	Clean zone	7	6.57
		2309-2316	Shaly zone	7	14.75
		2316-2320 (TD)	Clean zone	4	5.30

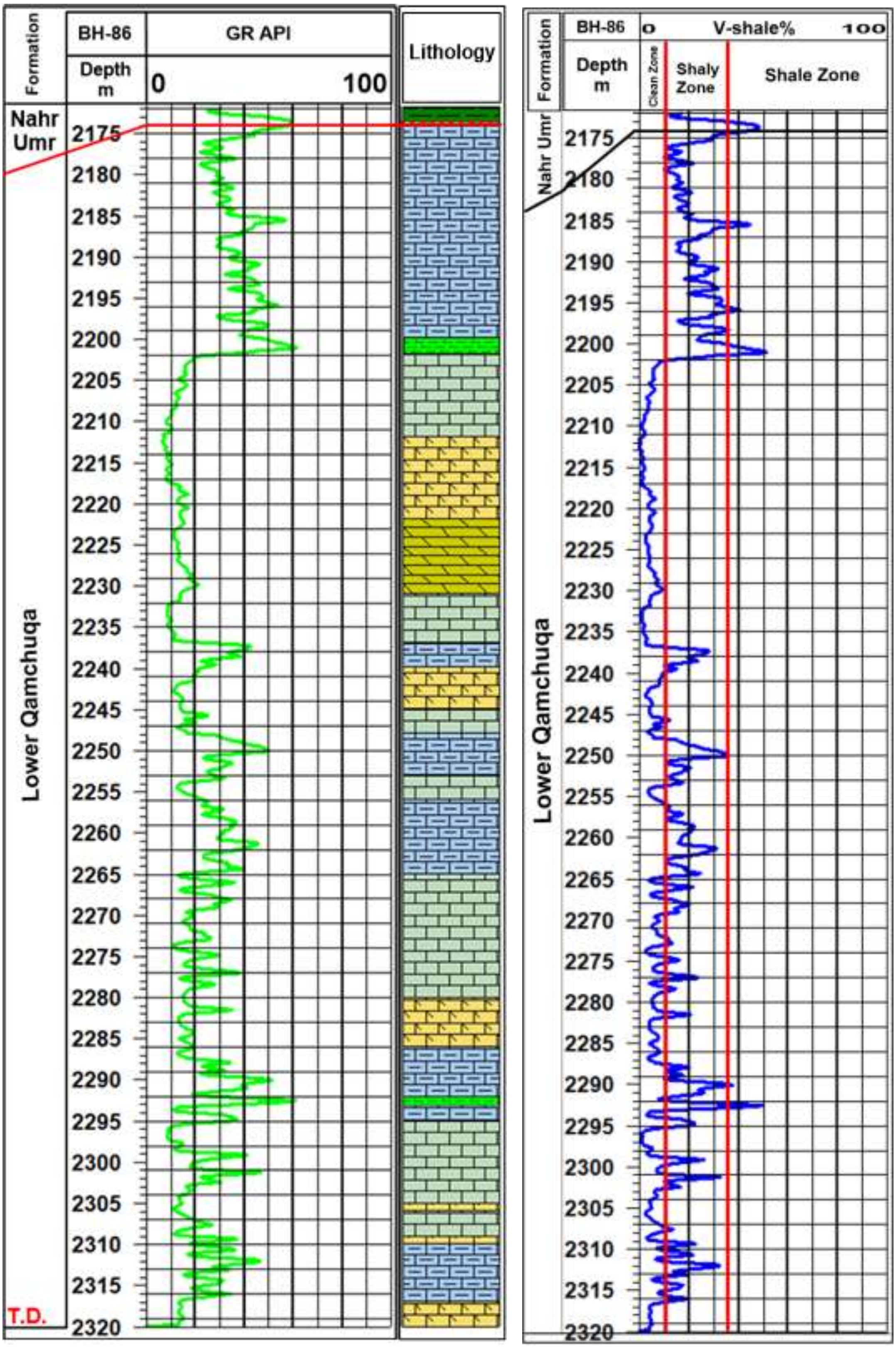

Figure 3- Gamma ray log and the calculated shale content for the Lower Qamchuqa Formation in the well BH-86.

d. Porosity Calculation

The calculated total neutron-density porosity (ΦN-D) is best representing the existed primary and secondary porosities which are mainly depended on the formation characteristics. The Neutron-density combination log can be calculated mathematically according to

Schlumberger, 1997 method [29]. The calculated ΦN-D porosity before and after correction from shale impact are shown in (Figure 4).

Most parts of the formation showed porosity values less than 15% except noticeable intervals in the middle part of the formation (between depths 2203m and 2235m), where low percentages of shale content coupled with porosity values exceeded 15%, (unusual high porosity values in some horizons of the formation in well BH-86 are not true porosity values as the density tool looks to be affected by the enlargements occurred in the borehole wall (Figure 4).

Generally, a gradual increase in porosity can be seen from the bottom of the section towards the top and up to the depth of 2204m, where a decrease in porosity and increase in the shale content starts towards the contact with the overlaid Nahr Umr Formation.

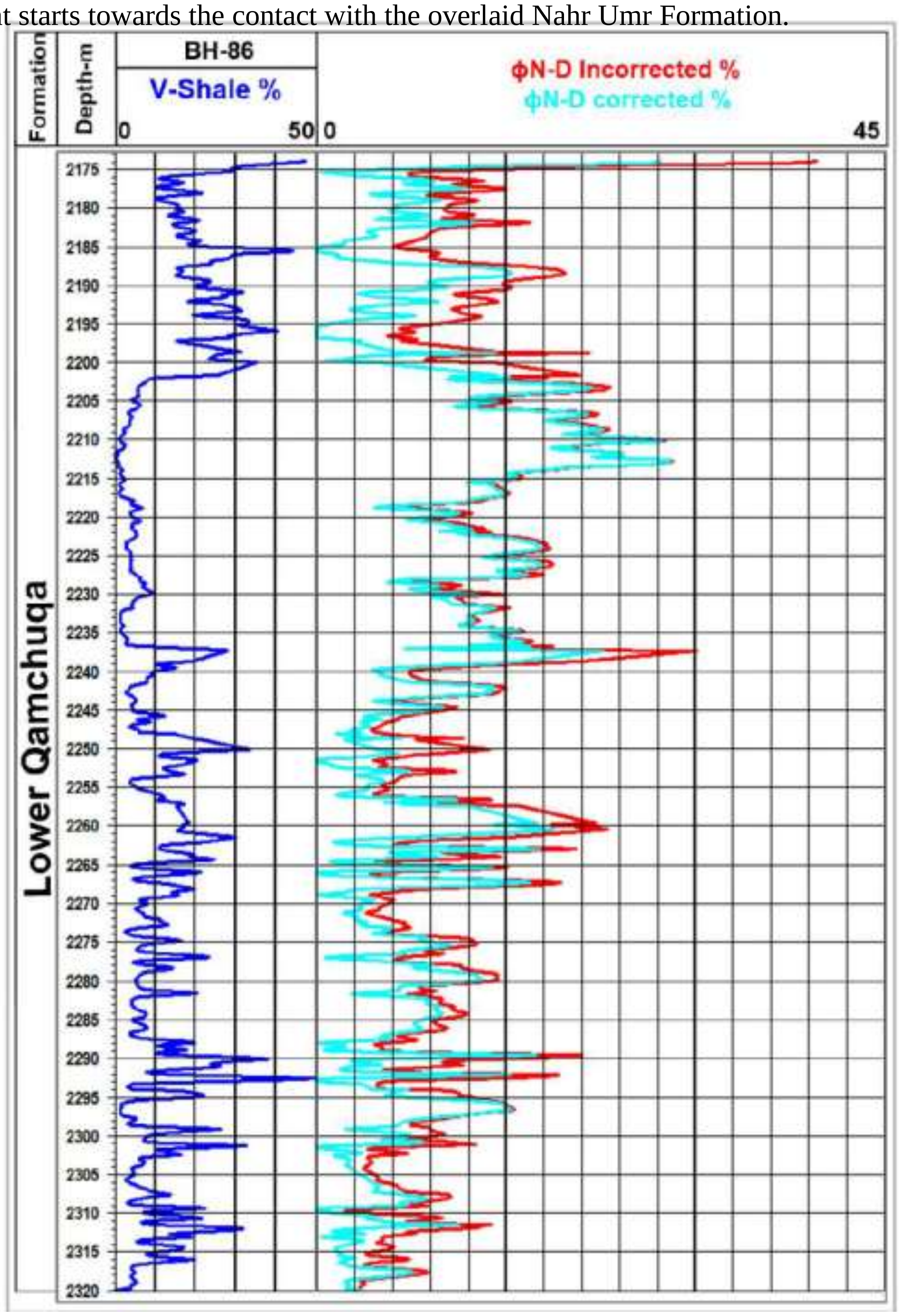

Figure 4- Incorrected and corrected Neutron - Density porosity (Φ_{N-D}) from shale impact for the Lower Qamchuqa Formation in the well BH-86.

e. Secondary Porosity

In order to determine the percentages of the secondary porosity (fractures or vugs), the difference between the corrected sonic porosity values (Φ_{Scor}) and the corrected neutron - density porosity values ($\Phi_{N\text{-}Dcor}$) calculated and plotted as a curve (Figure 5). It is well known that Φ_S is generally representing primary (matrix) porosity, whereas $Ø_{N\text{-}D}$ is a record of the total porosity, so the difference between both should represent the value of the secondary porosity. To avoid exaggeration in calculating values for the secondary porosity; the record of the Caliper log was also plotted (Figure 6).

Depth intervals are suffering from severe enlargement of the borehole wall that shows mistakenly high percentages of secondary porosity due to the mud effect on the logging tools. Accordingly, secondary porosity of less than 6% is expected to be contributed to the total porosity along the formation. The exceptionally calculated high secondary porosities are due to bad borehole wall conditions.

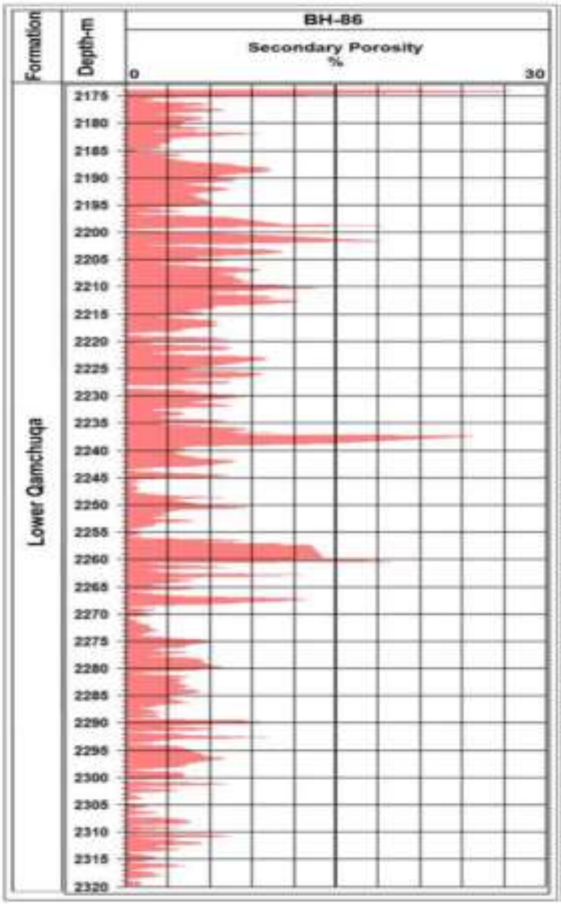

Figure 5- Detected secondary porosity for the Lower Qamchuqa Formation in the well BH-86.

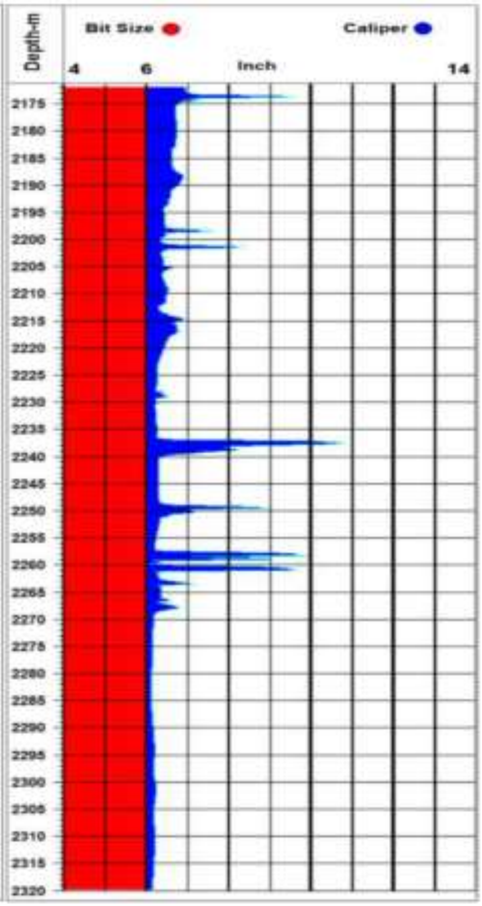

Figure 6- Record of the Caliper log for the Lower Qamchuqa Formation in the well BH-86.

f. Detection of Gas Bearing Zones

The zones in which their pores are filled with gas rather than oil or water start showing underestimated neutron porosity. This happens because the hydrogen index of gas is lower than of oil or water. Such a lower concentration of hydrogen confuses the neutron log tool and leads the tool to record a lower account of hydrogen atoms which is finally mistakenly interpreted as low porosity.

In contrast to the neutron log, the density log overestimates the porosity values in gas-bearing zones. This occurs as a result of being gas of less electron content in comparison with oil or water. Accordingly, for detecting gas-bearing horizons the log interpreter should overlay both neutron porosity and density porosity (or bulk density) curves and watch the zones in which obvious separation occurs between both curves. Such a separation is known in some literatures as "balloon shape" (zones in which low neutron porosity with high-density porosity recorded) [30].

In this study, and as an attempt for detecting gas zones in the Lower Qamchuqa Formation in the studied well, both curves of Φ_{Ncor} and Φ_{Dcor} were plotted as an overlay on the same track (Figure 7).

Gas bearing zones were detected at the upper part of the formation. The formation looks to be containing gas from its top to about a depth of 2200m in the studied well. The separations between the two curves become less in the deeper parts indicating more likely to the existence of relatively light oil-bearing zones.

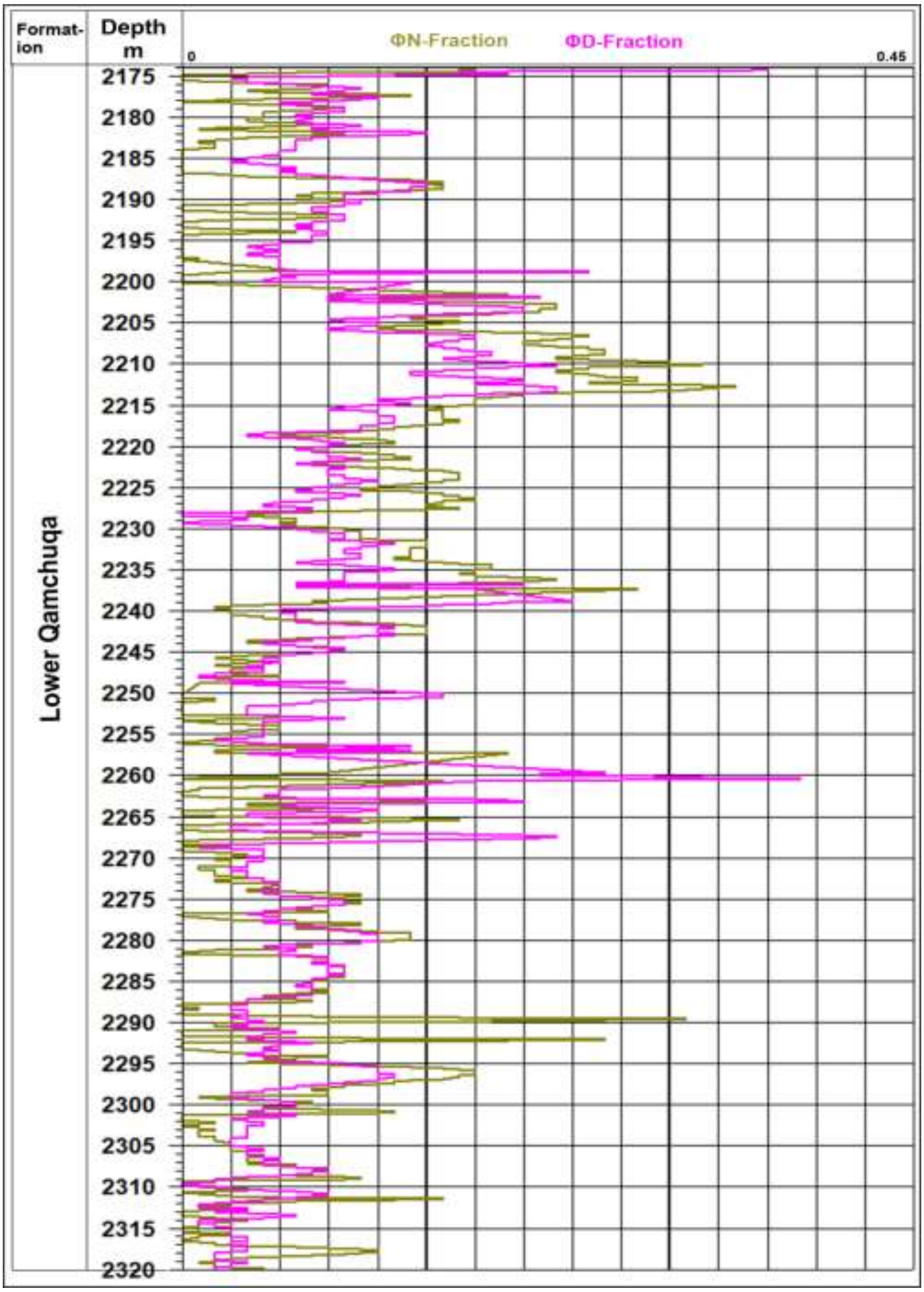

Figure 7- Neutron and Density porosity curve's crossover as appeared for Lower Qamchuqa Formation in the studied well of BH-86.

g. Permeability

The permeability can be measured directly from core test in the laboratory or indirectly can be estimated depending on some logging tools such as Caliper and SP logs. Nuclear Magnetic Resonance (NMR) considers one of the best logging tools which has the ability to measure permeability in millidarcies directly from the borehole.

In the present study, the permeability data from the core test was available for selected intervals. In an attempt to obtain permeability in millidarcies for the whole studied section of Lower Qamchuqa Formation, the Multiple Linear Regressions (MLR) method was used by taking benefit from the existed permeability values obtained from the core tests. The MLR method extends from the regression analysis, which integrates independent values for predicting a dependent value [31]. In this case, the predicted permeability values from the log data deem as dependent values in contrast to the well log data which consider as independent values.

In the present study, the gamma-ray, density, neutron, and sonic logs data are used as independent values to predict the dependent permeability value for each corresponded depth (Fig. 8A). Mohaghehet, et al., 1997 [31] believed that the following Eq.1 is the best in representing the relationship between permeability and the recorded log values.

$\text{Log (K)} = -11.577 + (0.0246*Gr) + (4.585*\rho b) + (0.112*\phi N) + (-0.027*\Delta t)$ Eq.1

Values for permeability obtained for the whole studied section through applying Eq.1 and plotted as a curve are shown in Figure 8B.

Most parts of the formation showed permeability values of less than 1.0mD. Values between 1.0 and 4.0mD only appeared to be existing in depth interval 2184m-2202m and in a number of narrower zones distributed along the section. The formation also included zones of extremely low permeability (<0.01mD).

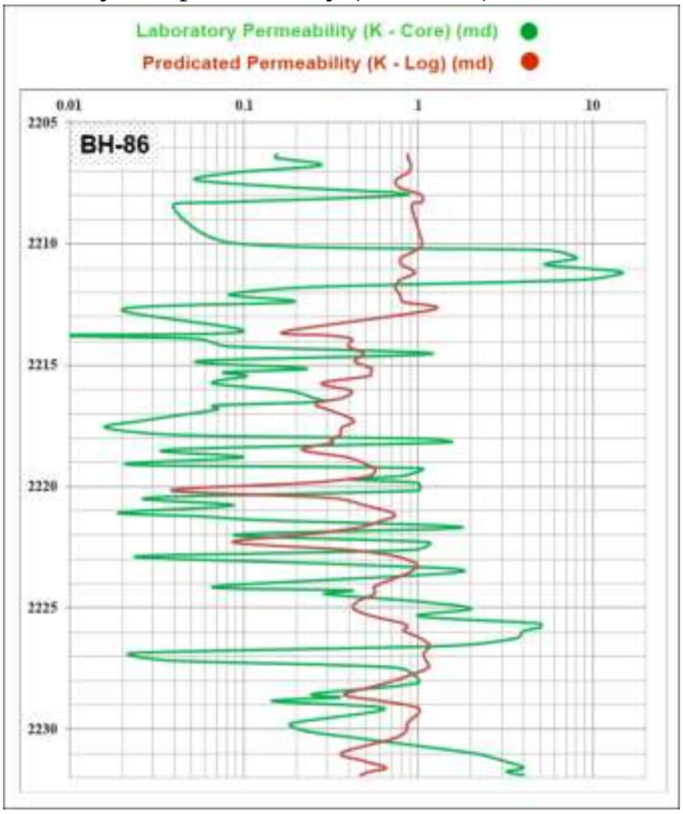

Figure 8A- Measured permeability from core test (green line) and the calculated permeability from log data using equation (red line) for the Lower Qamchuqa Formation in the well BH-86.

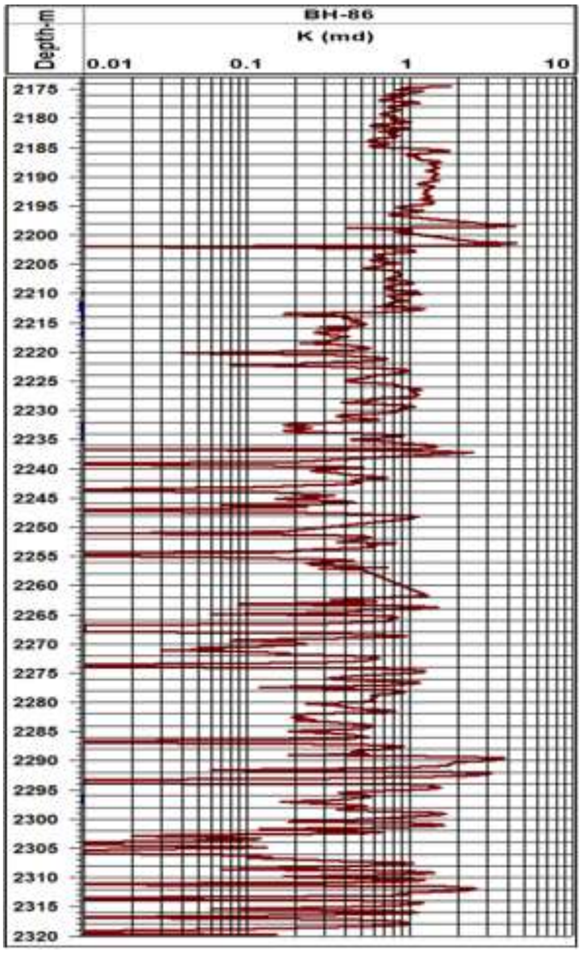

Figure 8B- Calculated permeability for the Lower Qamchuqa Formation in the well BH-86.

g. Reservoir Units

As shale content, porosity, and permeability values are calculated. Distinguishing between units with different reservoir properties can be done regardless to the type of fluid that stored in the reservoir. The reservoir units are distinguished in Lower Qamchuqa Formation in the studied well BH-86 depending on the correlation and the variation in the mentioned three parameters (Figure 9).

The 146m of the formation penetrated by the well BH-86 subdivided to six main reservoir units (RU) with further subdividing RU-2 to two sub-units.

Depth interval, thickness, statistics of shale content, porosity, permeability, and the common lithology of each reservoir unit are summarized in the Table 5.

Table 5- Depth interval, thickness, and a summarization for the properties of the identified reservoir units of the Lower Qamchuqa Formation in the well BH-86.

reservoir Units		Depth Interval (m)	Thick-ness (m)	Statistics	V_{Sh} (%)	Porosity (%)	Permeability (mD)	Main Lithology
RU-6		2174-2202	28	Min Max Average	8.49 47.69 22.98	0 27.19 6.15	0.001 4.46 1.11	Limestone & Shaley Limestone
RU-5		2202-2217	15	Min Max Average	0.00 8.21 2.87	10.32 28.04 18.70	0.17 1.22 0.72	Shaley Limestone & Marl
RU-4		2217-2236	19	Min Max Average	0.99 9.47 4.05	1.08 16.00 10.62	0.04 1.16 0.58	Limestone
RU-3		2236-2268	32	Min Max Average	2.49 33.69 11.51	0 22.73 7.17	0.001 3.68 0.45	Limestone , Dolomitic Limestone, & Dolomite
RU-2	B	2268-2288	20	Min Max Average	2.29 23.47 8.42	0.06 13.04 6.50	0.001 1.23 0.45	Limestone, Shaley Limestone, & Dolomitic Limestone
	A	2288-2302	14	Min Max Average	1.17 49.98 14.19	0 17.34 6.51	0.001 3.77 0.99	Shaley Limestone & Limestone
RU-1		2302-2320	18	Min Max Average	0.00 32.00 9.48	0 11.19 3.64	0.001 2.56 0.50	Shaley Limestone & Limestone

As a preliminary evaluation, RU-5 looks to be of the highest reservoir property among the distinguished reservoir units of Lower Qamchuqa Formation and that is due to the low shale content and relatively high porosity with the permeability around or greater than 1.0 mD. On the other hand, reservoir units RU-1, RU-2B, and RU-3 are of the lowest reservoir properties because of their low porosity and permeability.

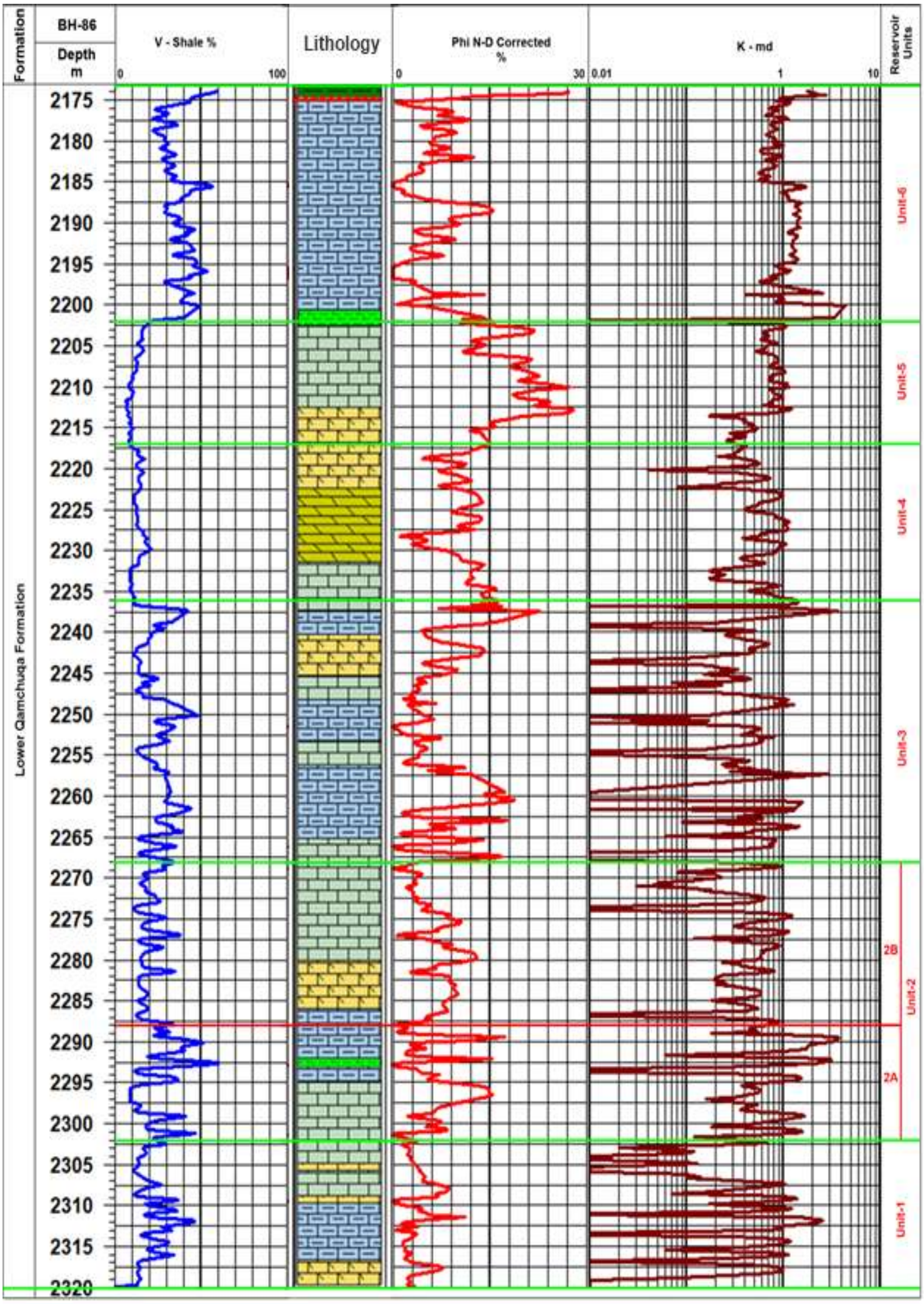

Figure 9- Identified reservoir units based on shale content, porosity, and permeability for the Lower Qamchuqa Formation in the well BH-86.

h. Water and Hydrocarbon Saturations

Usually, the records of the resistivity logs are presented as three curves on a logarithmic scale representing shallow, medium, and deep reading resistivity (Rxo, Ri, and Rt respectively). The separation or non-separation between the mentioned curves with respect to the nature of the used drilling mud (fresh or salt mud) will aid very well in detecting the nature of the reservoir fluids.

In the present study, the resistivity data were from Micro Spherical Focused Log (MSFL), Shallow Laterolog, (LLS), and Deep Laterolog, (LLD) by which Rxo, Ri, and Rt were recorded respectively for the studied Lower Qamchuqa Formation (Figure 10).

By following the mode of the plotted curves, horizons with non-separation or with separation by variable space widens can be seen (Figure 10).

As fresh mud is used during the drilling operation of the studied well, so non-separation between the resistivity curves is the most interesting mode that should be followed in the studied section. Non-separated Rxo and Rt curves will be an indication of hydrocarbon-bearing zones as fresh mud filtrate and hydrocarbons are both non-conductive materials.

Attention should be paid also to the resistivity values even in the non-separated resistivity curve conditions. Hydrocarbon-bearing horizons with low porosity are generally of higher resistivity values (more rock materials), whereas hydrocarbon-bearing horizons of high porosity are of relatively lower resistivity values (fewer rock materials). Accordingly, the best productive parts of the Lower Qamchuqa Formation in this study are expected to be the zones in which the resistivity curves are showing no separation with relatively low recorded resistivity values.

Water saturation (Sw) determination is the most challenging and important process of petrophysical parameter calculations.

The importance of water saturation determination is in being the parameter that can be determined by the logging data which contributes in determining the hydrocarbon saturation (Sh) through the simple equation of 1.0 – Sw.

The calculated water saturation values by Archie's equation for the Lower Qamchuqa Formation in the studied well needed a value for the cementation exponent (m) which has been determined through Pickett crossplot method and appeared to be equal to 1.61 (Figure 11).

The calculation of water saturation values within the flushed zone (Sxo) and uninvaded zone (Sw) is aided in further calculating residual hydrocarbon saturation (Shr) and movable hydrocarbon saturation (Shm) by applying Eq.2 and Eq.3 respectively.

$$\text{Residual hydrocarbon saturation (Shr)} = 1.0 - \text{Sxo} \quad \text{(Eq.2)}$$

$$\text{Movable hydrocarbon saturation (Shm)} = \text{Sxo} - \text{Sw} \quad \text{(Eq.3)}$$

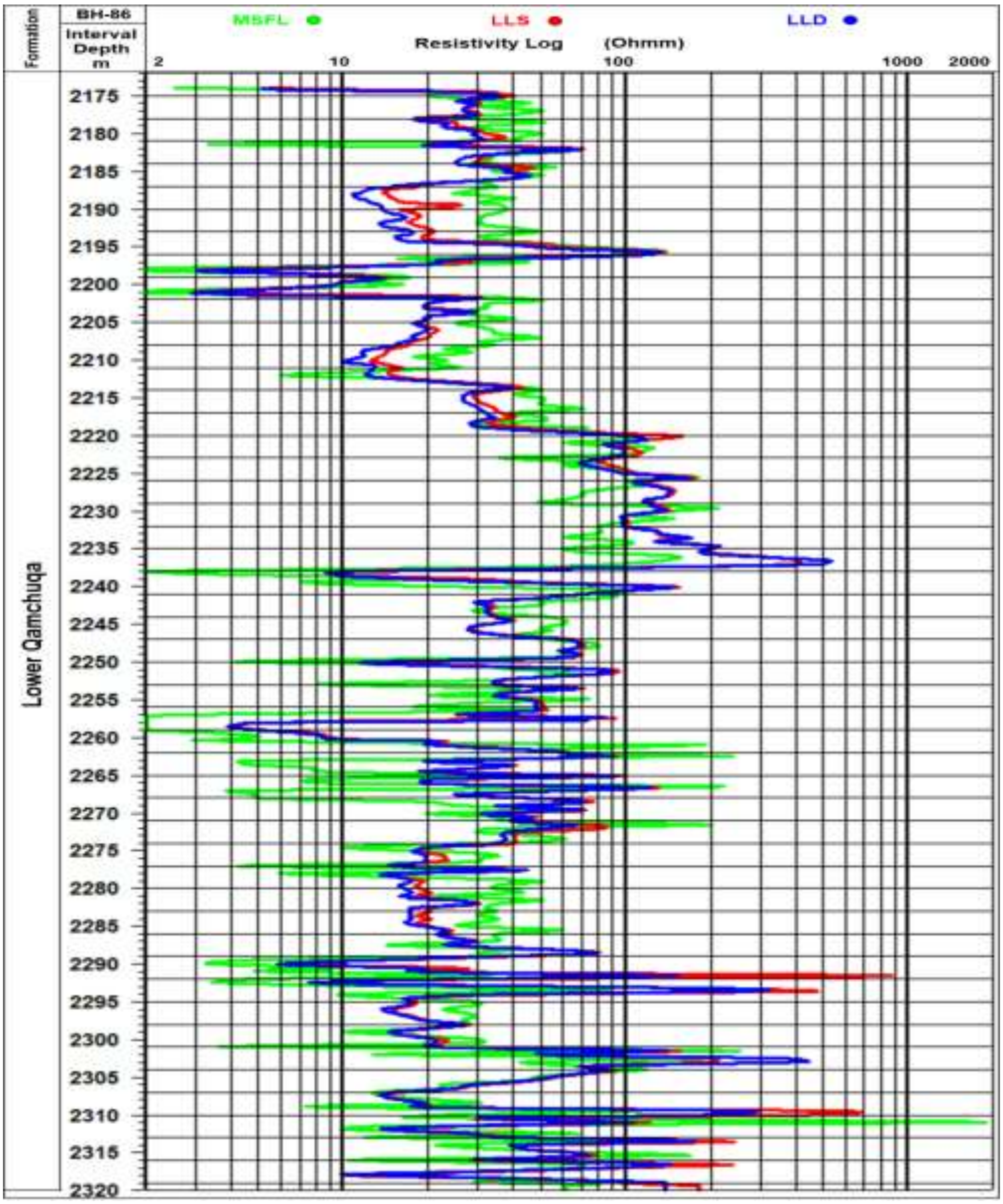

Figure 10- The recorded resistivity logs for the Lower Qamchuqa Formation in the

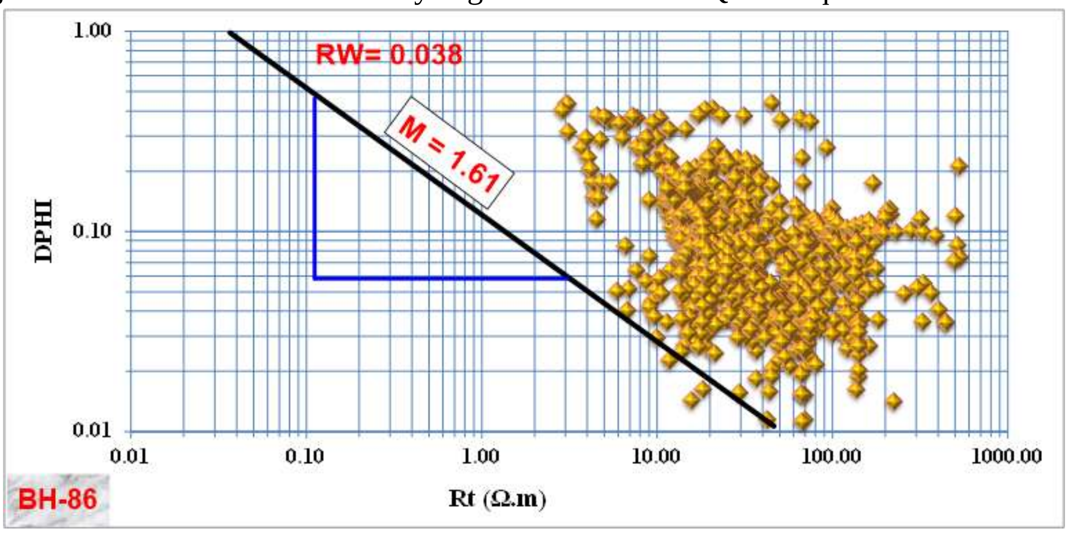

Figure 11- Determination of the value of Cementation exponent (m) by Pickett crossplot for the Lower Qamchuqa Formation in the well BH-86.

Figure 12 shows the distribution of the mentioned three saturations as percentages within the pore spaces of the Lower Qamchuqa Formation in the studied well.

Movable hydrocarbons (even with small percentages) can be observed along the studied section. The highest residual hydrocarbons are concentrated in the reservoir units RU-4 to RU-6. The combination of relatively high porosity and high percentages of residual hydrocarbon saturations is an indication to the existence of numerous tiny or separated pore spaces.

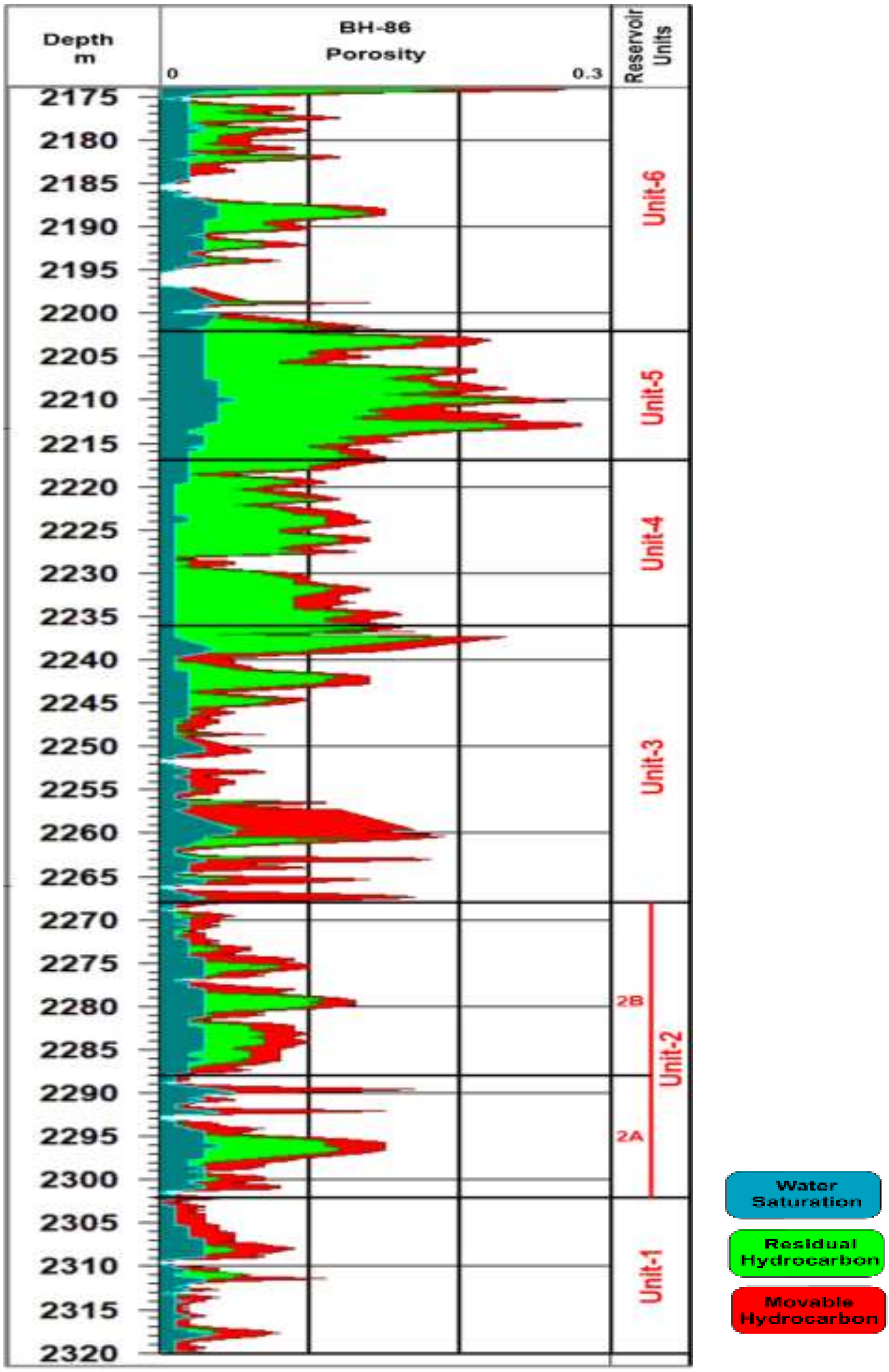

Figure 12- Water, residual hydrocarbon, and movable hydrocarbon saturations within the porosity of the Lower Qamchuqa Formation in the well BH-86.

i. Bulk Volume Water (BVW)

The Bulk Volume of Water (BVW) can be defined in log analysis as the fraction of rock volume which is occupied by the water and mathematically is expressed as the product of the formation's water saturation (Sw) multiplied by porosity (Ø).

BVW has many important applications within a particular reservoir. When BVW is calculated at several depths of a reservoir and values remain constant or very close to constant, that will be an indication of being the reservoir at irreducible water saturation (Swirr) condition [30].

Moreover, Buckles, 1965 plot [32] is a graph of porosity versus water saturation proposed by Humbolt, 2006 [33]. This crossplot is applied to detect which reservoir unit of the Lower Qamchuqa Formation in the studied well is in or near irreducible water saturation condition and which is not (Figure 13).

Reservoir unit RU-6 of Lower Qamchuqa Formation showed sample point distribution almost around one single hyperbolic line which means that this reservoir unit may produce water-free hydrocarbons or with a low quantity of water (if there are hydrocarbons in the unit).

Although RU-5 is relative of higher porosity than the other reservoir units; it showed more heterogeneous properties as its sample points scattered around more than two hyperbolic lines indicating to the probability of production with a high ratio of water.

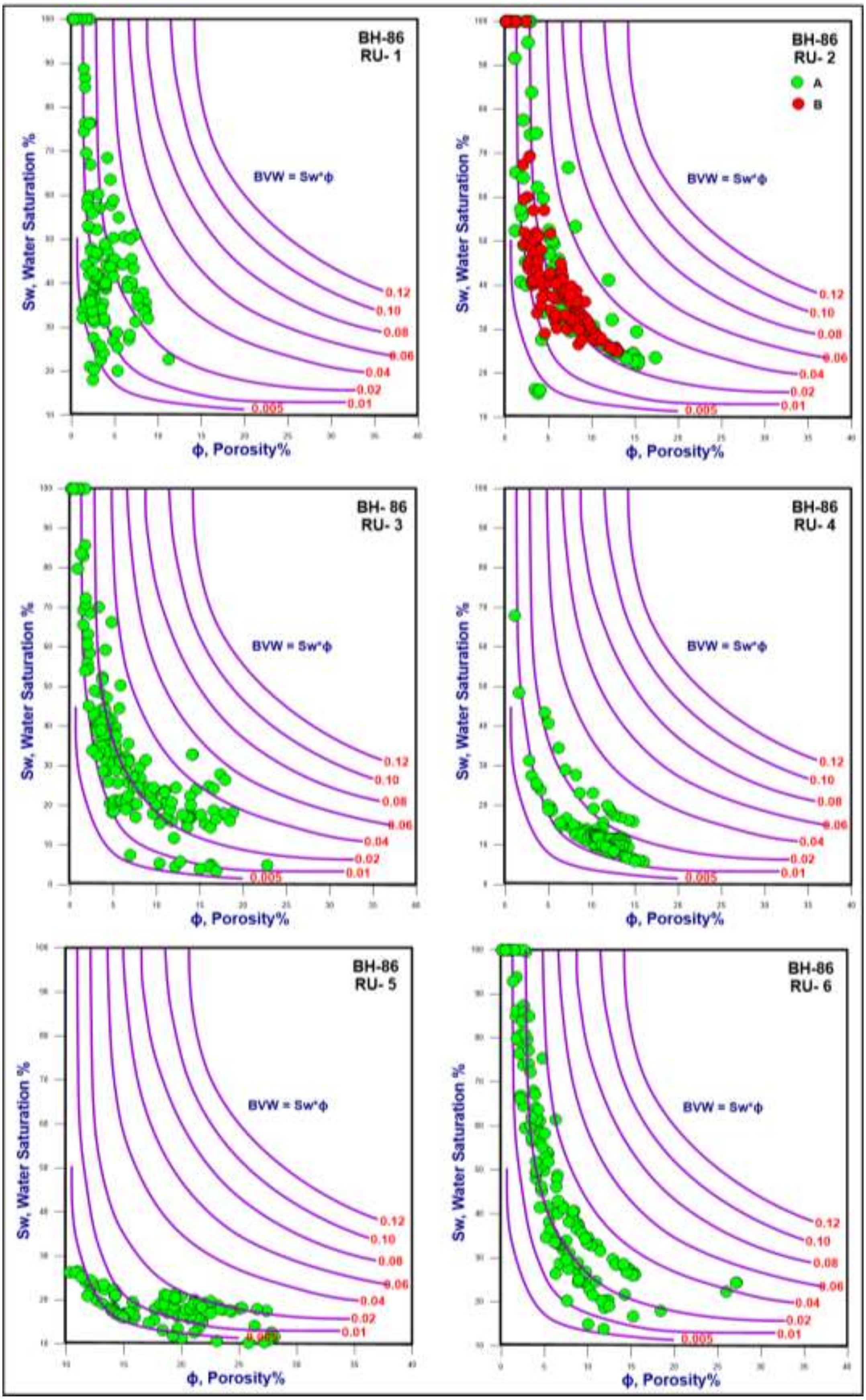

Figure 13- Porosity versus water saturation on Buckles plot to show BVW values for the reservoir units of the Lower Qamchuqa Formation in the well BH-86.

Both reservoir units RU-3 and RU-4 seem to be somehow homogeneous units as their sample points are distributed around one or two hyperbolic lines with non-observable randomly scattering points. The same is true with the reservoir units RU-2 A and B except a few points looked to be departed from other sample points indicating to kind of heterogeneity in the saturations.

The reservoir unit RU-1 showed the highest heterogeneity among the distinguished reservoir units by being their points distributed around more than three hyperbolic lines indicating variations in the BVW values and hence expectation for this unit is a production with a high quantity of water.

j. Fluid Flow

From the relationship between porosity and permeability proposed by Amaefule, et al., 1993 [34], an attempt is done to detect the flow type in the studied Lower Qamchuqa Formation.

The flow is generally expected to occur either due to permeability through fractures, fractures and matrix, or essentially matrix.

The distribution of the sample points for the recognized reservoir units in the present study are determined (Figure 14). The effective contribution of fractures in flowing can be seen in most of the reservoir units in the studied well.

The less contribution of the fractures with matrix porosity is in the RU-4 and RU-5. It is important to mention that although fractures are contributed to supporting the permeability but still the pore throats and avenues are of very small sizes (less than 1.0 micron).

Teh, et al.,2011 [35] introduced FZI as a parameter that is inversely related to those critical factors determining the flow in the rock, namely the shape factor, tortuosity, and grain surface area. As the FZI value discriminates the pore geometry of reservoir rock into flow zones, therefore the high FZI value is expected to be indicating that the rock is of well-sorted and coarse grains with a lower shape factor. A lower FZI value on the other hand will indicate to a rock constituent of fine and poorly sorted grained [36]. The technique of calculating FZI from core data is applied in this research [35]. This technique involves normalized porosity index (Φz) and reservoir quality index (RQI) as shown in Eq.4. to Eq.6 [35].

$$FZI = RQI / \Phi_Z \qquad \text{(Eq.4)}$$
$$\Phi z = \Phi e / (1-Øe) \qquad \text{(Eq.5)}$$
$$RQI = 0.0314\ (K/\Phi e)^{½} \qquad \text{(Eq.6)}$$

Where:
FZI: Flow Zone Indicator.
RQI: Reservoir Quality Index.
Φz: Normalized Porosity Index.
K = Permeability in mD.
Φe = Effective porosity in fraction.

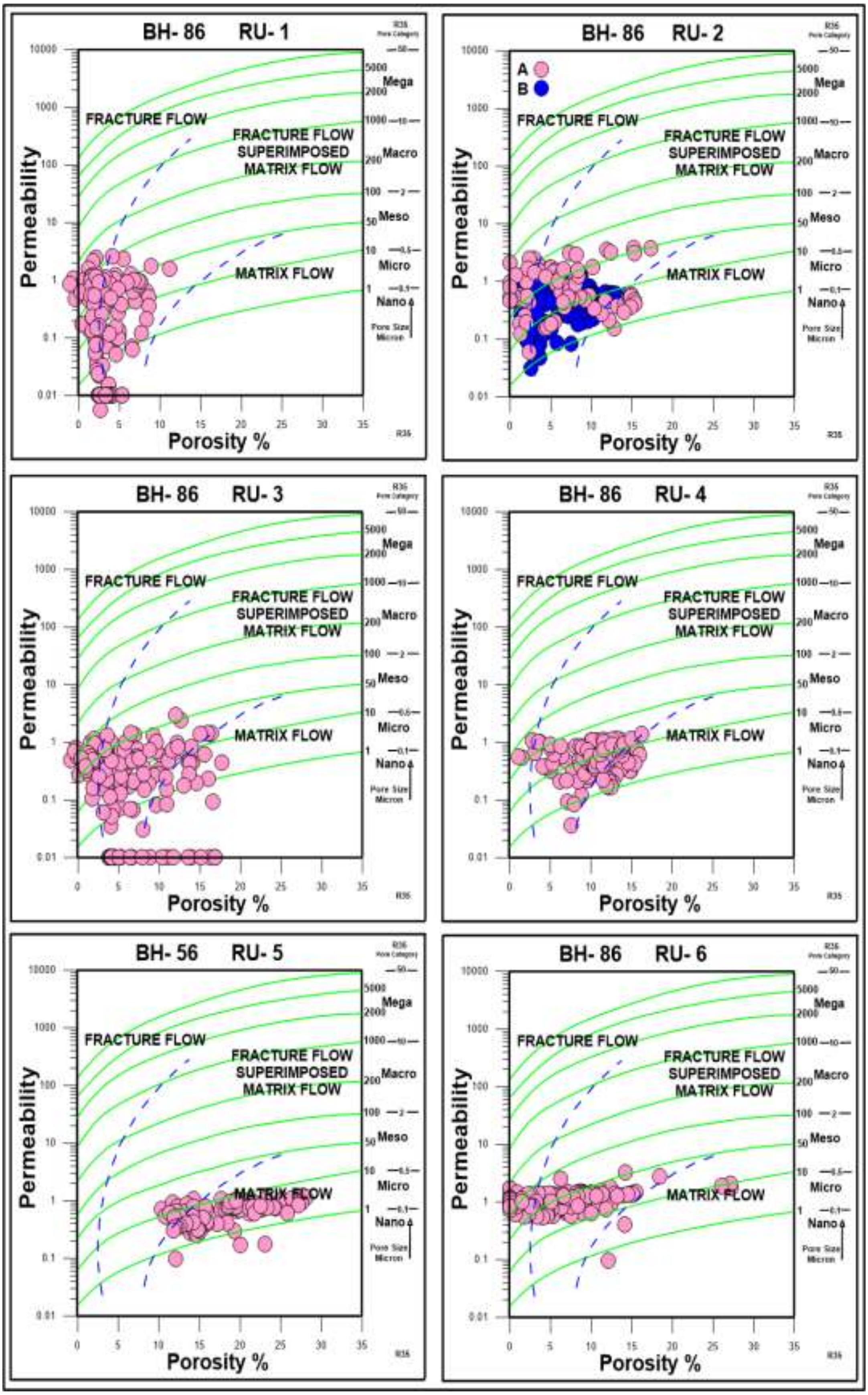

Figure 14- Porosity - permeability crossplots showing the type of flow and pore throat sizes for the reservoir units of the Lower Qamchuqa Formation in the well BH-86.

Any zone of certain FZI value is a representative zone of characteristic Hydraulic Flow Unit (HFU). The flow unit can be defined as a reservoir zone which has lateral and vertical continuity within the same porosity (Φ) permeability (K) and bedding characteristic [36] [37].

The calculated FZI values for Lower Qamchuqa Formation are displayed in Figure 15. Normal probability index was used to distinguish between the variable FZI populations (groups).

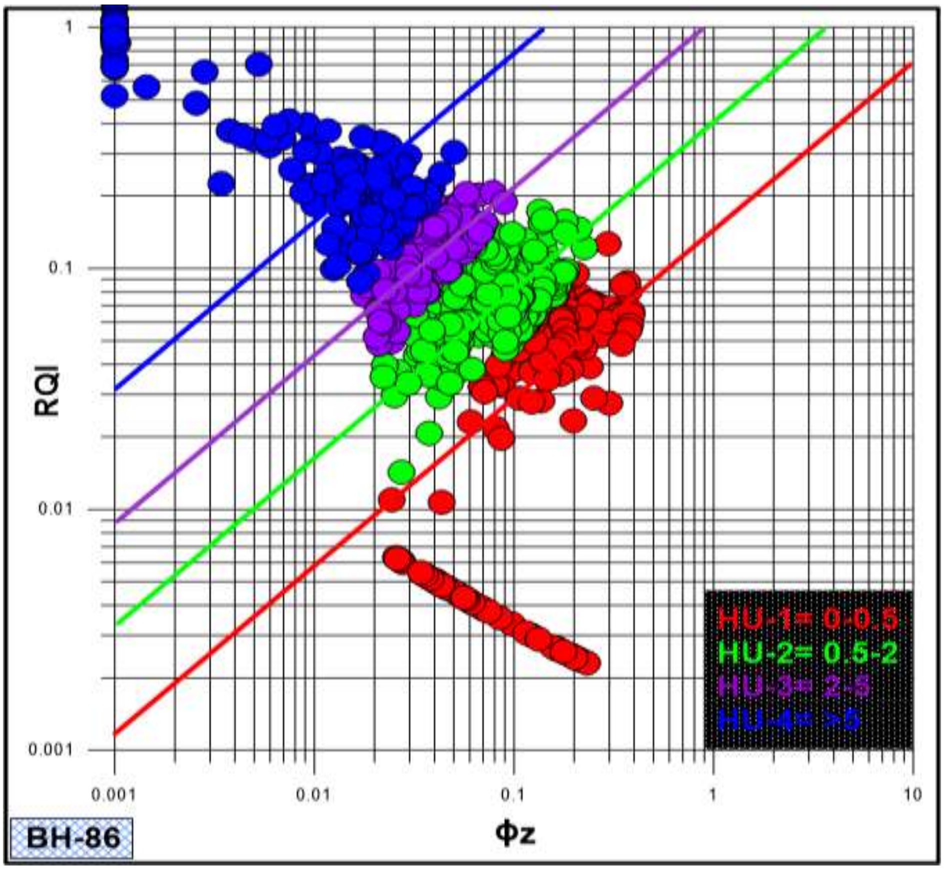

Figure 15- The identified HFUs using FZI technique for the Lower Qamchuqa Formation in the well BH-86.

Four populations of FZI values recognized depending on the change in the slope of the trend lines for the distributed FZI sample points. So, Lower Qamchuqa Formation in the studied well looks to own four unique HFUs with the FZI ranges and average values are shown in the Table 6.

Table 6- Ranges and averages of the calculated FZI and HFUs of the Lower Qamchuqa Formation in the well BH-86.

Wells	FZI Range	Average FZI	Hydraulic Flow Units
BH-86	0-0.5	0.28	HU-1
	0.5-2	1.03	HU-2
	2-5	3.06	HU-3
	>5	205.77	HU-4

k. Movable Hydrocarbon Index (MHI)

The Movable Hydrocarbon Index (MHI) is used as one of the quick look methods (QLM) to estimate the movability of the hydrocarbons. When the value of Sxo is greater than Sw then the hydrocarbons in the flushed zone have possibly been moved or flushed out of the zone nearest the borehole by the invading drilling fluids.

According to Schlumberger, 1972 [38], if the ratio of Sw/Sxo (MHI) is 1.0 or greater, then no movable hydrocarbons have occurred during the invasion, and this is true regardless of whether or not the zone contains hydrocarbons, and if the ratio of Sw/Sxo is less than 0.7 for sandstone and less than 0.6 for limestone, then movable hydrocarbons is detected. The reservoir with MHI less than 0.6 indicates the existence of hydrocarbons having enough permeability to move during the invasion process by the mud filtrate [39].

The calculated MHI values for the Lower Qamchuqa Formation in the studied well are drawn as a curve and shown in Figure 16. The MHI value of 0.6 was used as a cutoff value for separating the movable hydrocarbon zones from non-movable hydrocarbon zones.

Most parts of the formation in the studied well are containing movable hydrocarbons, especially RU-3 and RU-4. Narrow horizons of non-movable hydrocarbons intercalated the formation in the RU-1 and RU-2B.

Although, the FZI method aids in recognizing flow ability in a reservoir but it still can't give an idea about the nature of the fluids that flow. In order to connect the ability to flow and the flowed fluid type (water or hydrocarbons) in Lower Qamchuqa Formation; both MHI and FZI values are correlated (Figure 16). The best productive zones should be those intervals in which low MHI values (lower than 0.6) are coupled with high FZI values. Accordingly, RU-6 looks to be a promised productive interval. The RU-5 showed the least production capability due to weak flow ability. The rest of the reservoir units (RU-1 to RU-4) are containing a lot of productive horizons with different thicknesses and different flow abilities.

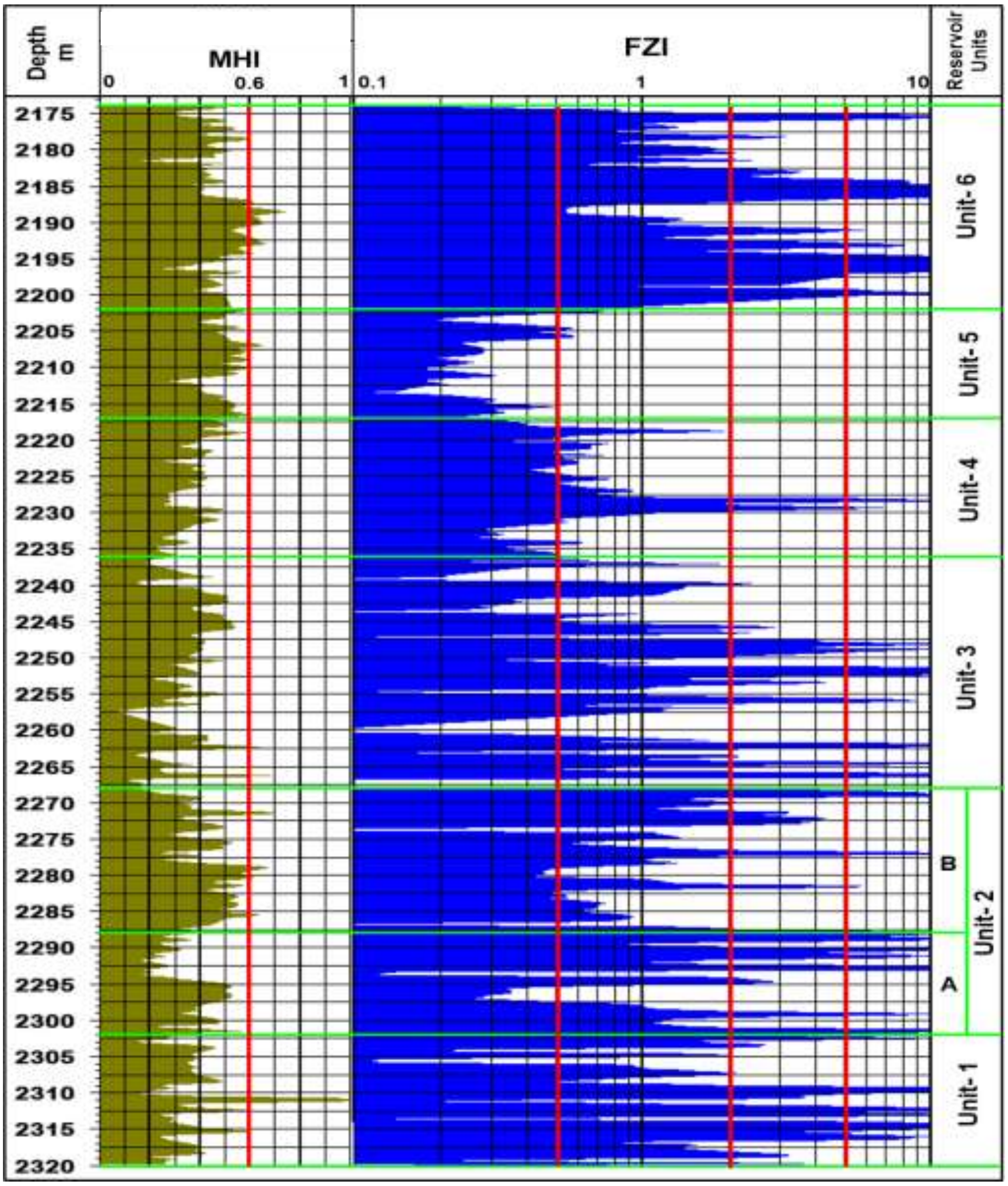

Figure 16- Correlation between the calculated MHI and FZI values of the Lower Qamchuqa Formation in the well BH-86.

In the same manner and for gas production the permeability cutoff of 0.1 mD considers

l. Net to Gross Reservoir and Pay Ratios

The significance of the terms “net-to-gross” (NTG) and “cut-offs” is ultimately to define productive zones in the reservoir for hydrocarbon exploitation. The geologist may be concerned with the pay for evaluating hydrocarbon in-place and the ultimate estimation of economically producible reserves [40].

In the present study, the gross thickness is the total thickness of the studied section from the Lower Qamchuqa Formation in the studied wells of BH-86 and is equal to 146m. Net reservoir thickness is the total thickness of the reservoir component referred to as having reservoir quality rock, the tight rock and shaley components inhibiting flow are filtered off, and the Vsh, Ø, and K cutoffs are applied.

Net pay thickness comprises those hydrocarbons bearing reservoir intervals that can produce economically, defined additionally by log-derived water saturation (Sw) cutoff. The thickness of the net production is considered to be the fraction of the net pay (reservoir) thickness that is subjected to the MHI cutoff to make sure about the productivity of the intervals. Accordingly, the ratios of the last three mentioned parameters can be computed in comparison with the gross thickness to determine N/G reservoir, N/G pay, and N/G productive ratios respectively.

In this study, the cutoff of shaleness of 35% confirmed to be agreeable for separating shale zones (of very low permeability) from clean and shaley zones (shaley zones could be of acceptable porosity and permeability).

Several authors are agreed with the minimum permeability cutoff of 1.0mD to distinguish between zones with effective fluid (oil) flow ability and zones of non or very low fluid flow capacity as an acceptable limit for production[41; 42 ; 43 ; 44 and 45]. In the present study, two scenarios are proposed to present for the cases of whether production of oil or gas. So, both mentioned permeability cutoffs of 0.1 and 1.0 mD are used to estimate the porosity and water saturation cutoffs for Lower Qamchuqa Formation (Figures 17 and 18; Table 7).

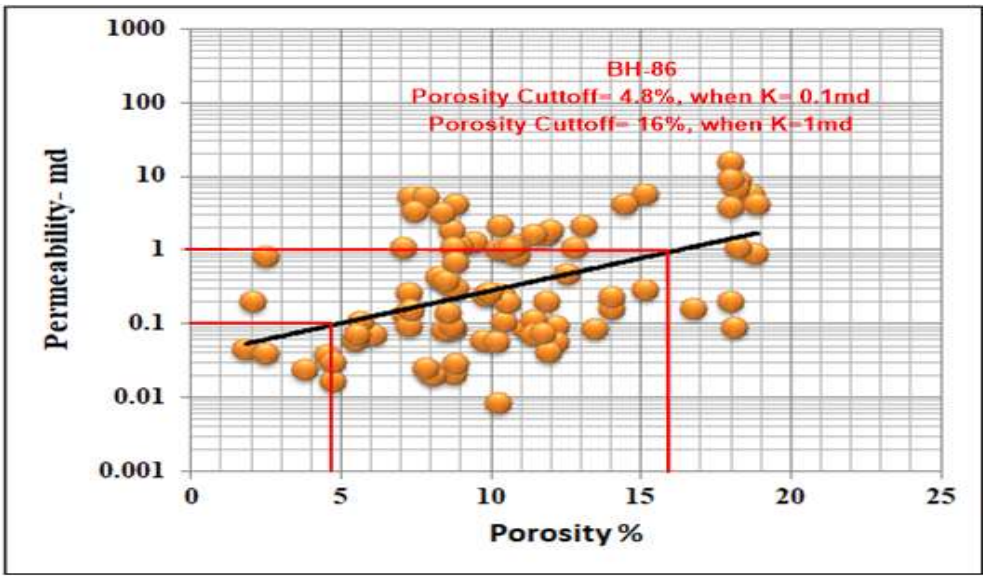

Figure 17- Porosity cutoff measurement for both cases of oil and gas for the Lower Qamchuqa Formation in the well BH-86.

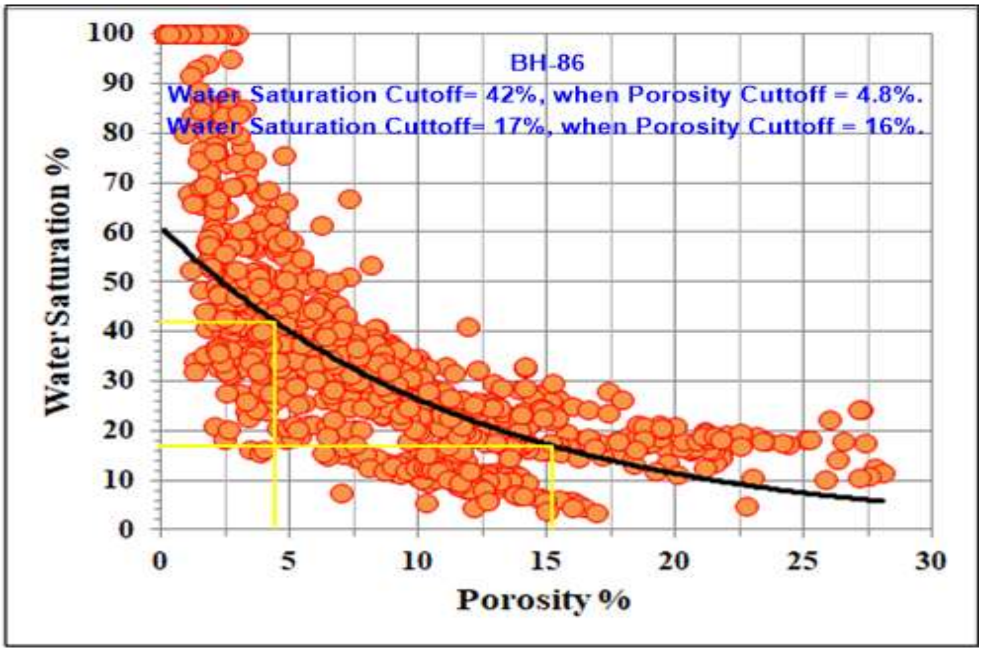

Figure 18- Water saturation cutoff measurement for both cases of oil and gas for the Lower Qamchuqa Formation in the well BH-86.

Table 7- The used cutoffs in calculating N/G values for both cases of oil and gas production for the Lower Qamchuqa Formation in the well BH-86.

Shale cutoff %	K cutoff mD	Ø cutoff %	Sw cutoff %	MHI cutoff
35	1.0 (oil)	16	17	0.6
	0.1 (gas)	4.8	42	

The calculated values included N/G reservoir (using Vsh, Φ, and K cutoffs), N/G pay (using Vsh, Φ, K, and Sw cutoffs), and N/G productive (using Vsh, Φ, K, Sw, and MHI cutoffs). The calculated different N/G values for the Lower Qamchuqa Formation in the well BH-86 in the case for oil production and the location of the best expected productive horizons of the formation for oil in the well were presented in Table 8 and Figure-19.

Table 8- Calculated N/G reservoir, pay, and productive ratios for the case of oil production for the Lower Qamchuqa Formation in the well BH-86.

Formatin	Reservoir Units	Gross Thick. (m)	Net Reservoir Thick. (m)	Net Pay Thick. (m)	Net Product. Thick. (m)	N/G Reservoir (%)	N/G Pay (%)	N/G Product. (%)
Lower Qamchuqa	6	28	0.0	0.0	0.0	0.0	0.0	0.0
	5	15	4	1.9	1.4	2.73	1.3	0.95
	4	19	0.0	0.0	0.0	0.0	0.0	0.0
	3	32	7.1	2.4	2.4	4.86	1.64	1.64
	2B	20	0.6	0.4	0.4	0.41	0.27	0.27
	2A	14	0.0	0.0	0.0	0.0	0.0	0.0
	1	18	0.0	0.0	0.0	0.0	0.0	0.0
Total		**146**	**11.7**	**4.7**	**4.2**	**8.0**	**3.21**	**2.86**

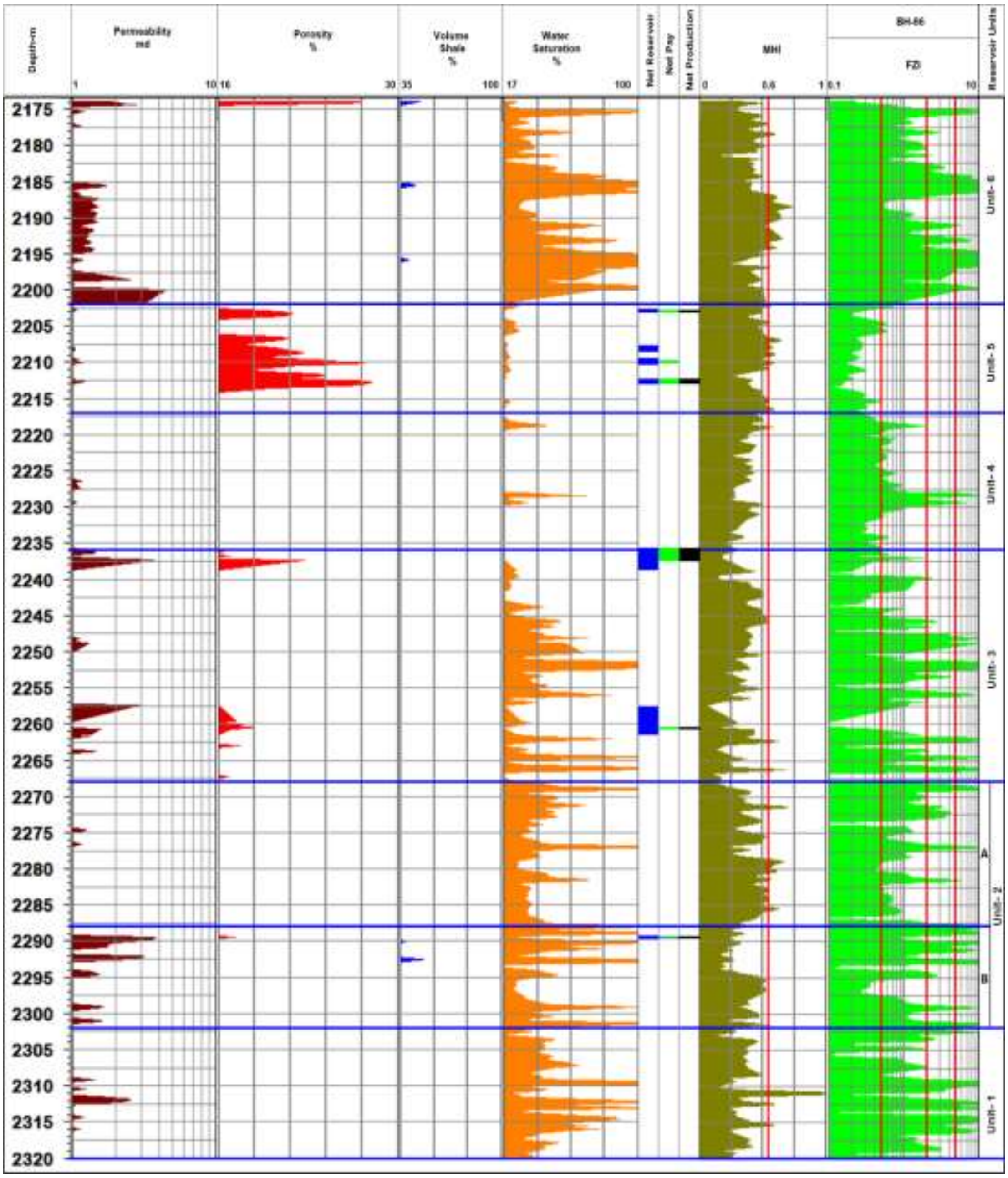

Figure 19- Net reservoir, pay, and productive zones for the case of oil production with the used cutoffs for the Lower Qamchuqa Formation in the well BH-86.

Only about 8% of the gross 146m of the formation is expected to be of the required reservoir properties for oil production. The payable thickness comprises about 3.2% of the gross formation's thickness and the actual productive thickness will be only about 2.8%.

As appears in Figure 19, all the promised horizons locate in the RU-3 and RU-5 (with a very small portion in the RU-2B) and the best productive horizon is the couple meters located at the uppermost part of the RU-3 where all the required reservoir (rock) properties coupled with required hydrocarbon saturation, movability, and relatively high FZI values.

For the case of gas production and by using the determined cutoffs for gas, the formation showed much more potential as a reservoir. The calculated N/G values listed in Table 9 indicate more than 68% of the gross thickness of the formation of acceptable reservoir

properties. More than 53% of the formation can be considered as pay and more than 50% as actual productive thickness from the gross 146m of the formation.
Generally, production is expected to be done from all the reservoir units with different potentialities. RU-3 looked to be the most potential reservoir unit followed by RU-4, whereas RU-1 at the lower part of the formation showed the least potentiality for gas production among the identified reservoir units.

Accordingly, a lot of depth intervals have the ability for producing gas but the depth interval between depths 2202 and 2245m looks to be the best as it shows more continuity as an interval without interrupting by effective non-productive horizons (Figure 20).

Table 9- Calculated N/G reservoir, pay, and productive ratios for the case of gas production for the Lower Qamchuqa Formation in the well BH-86.

Formation	Reservoir Units	Gross Thick. (m)	Net Reservoir Thick. (m)	Net Pay Thick. (m)	Net Production Thick. (m)	N/G Reservoir (%)	N/G Pay (%)	N/G Product. (%)
Lower Qamchuqa	6	28	17.8	9.45	5.8	12.19	3.97	3.97
	5	15	15	15	12	10.27	10.27	8.21
	4	19	19	17.3	17.3	12.32	11.84	11.84
	3	32	22.8	20.28	20.28	15.61	13.89	13.75
	2A	20	13.4	10.9	10.2	9.17	7.46	6.98
	2B	14	8.55	5.75	5.75	5.85	3.93	3.93
	1	18	4.55	2.6	2.05	3.11	1.78	1.4
Total		**146**	**100.1**	**81.28**	**73.18**	**68.52**	**53.14**	**50.08**

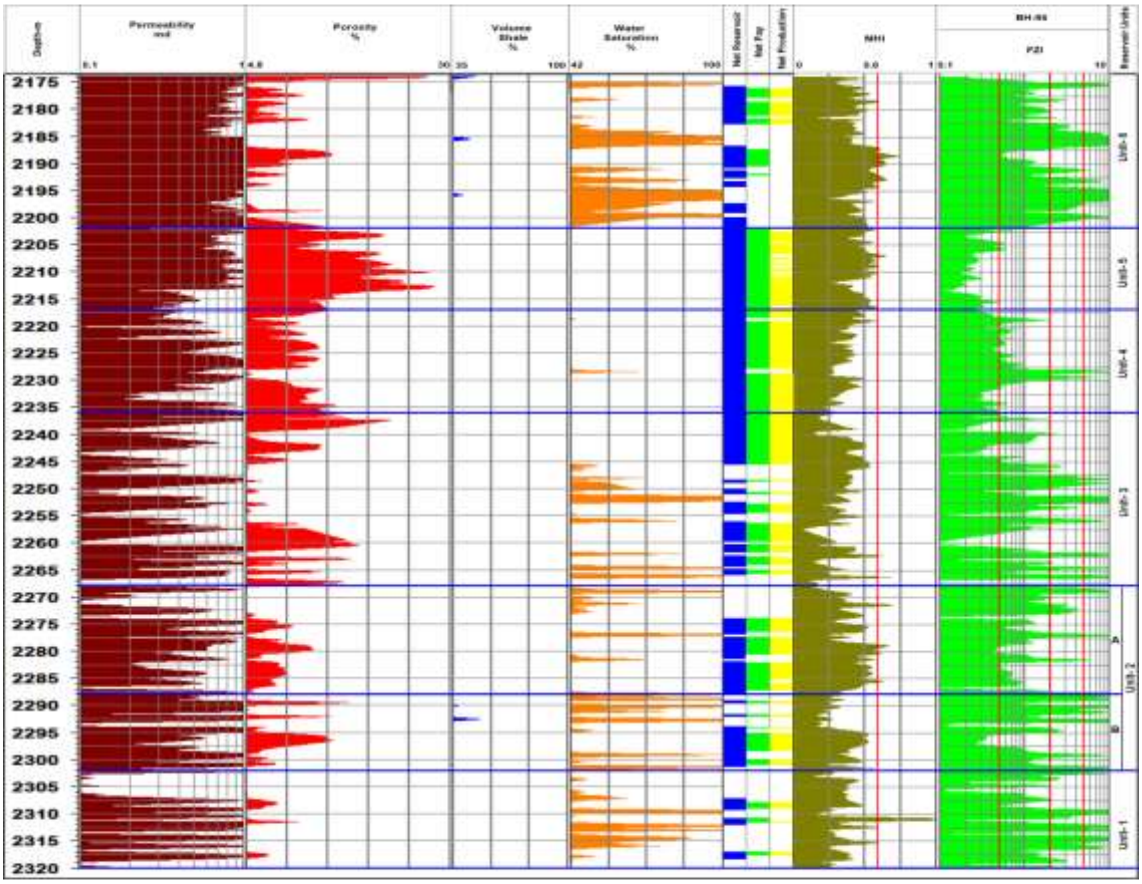

Figure 20- Net reservoir, pay, and productive zones for the case of gas production with the used cutoffs for the Lower Qamchuqa Formation in the well

4. Conclusions

The main conclusions are summarized as follows:

- Depending on the petrographic study, gamma-ray log, and calcimetry test; the upper part of Lower Qamchuqa Formation in well BH-86 of Bai Hassan Field looks to be composed of shaley limestone, limestone, dolomitic limestone, interbedded occasionally with thin beds of marl. Whereas, the middle and lower part of the formation are composed of dolomite, shaley limestone, dolomitic limestone, and limestone.
- Four main microfacies were recognized, Lime mudstone microfacies, Dolomudstone facies, Lime wackestone microfacies (subdivided into benthonic foraminiferals lime wackestone submicrofacies and bioclasts lime wackestone submicrofacies), and *Orbitolina* lime packstone microfacies (subdivided into pelloidal lime packstone submicrofacies and *Orbitolina* lime packstone submicrofacies).
- The paleo-depositional environment of the Lower Qamchuqa Formation in the studied area is the restricted and shallow open marine environment (interior platform).
- The formation (depending on petrophysics and log analysis study) is of relatively low shale content (<35%), except for some horizons at the upper part of the formation.
- The formation generally has porosities between less than 1.0 and 15% with a contribution from the second type porosities reaches to about 6% of the total porosity in some intervals.
- The permeability of the formation is generally low ranging mostly between less than 0.01 and 2.0mD.
- Almost the whole parts of the formation in the well BH-86 is containing hydrocarbon with different saturations.
- The fluids within the Lower Qamchuqa Formation in the studied wells are flowing as four hydraulic flow units with different average FZI values.
- Only about 8% of the gross 146m of the formation (in the well BH-86) is expected to be of the required reservoir properties for oil production. The payable thickness comprises about 3.2% of the gross formation's thickness and the actual productive thickness is only about 2.8%.

- For the case of gas production; 68% of the gross thickness of the formation is of acceptable reservoir properties. More than 53% of the formation can be considered as pay and more than 50% as actual productive thickness from the gross 146m of the formation.
- A lot of depth intervals from Lower Qamchuqa in the well BH-86 have the ability for producing gas but the depth interval between depths 2202 and 2245m looks to be the best as it shows more continuity as an interval without interrupting with effective non-productive horizons.

Acknowledgements

The authors would like to thank very much the geological staff of the Northern Oil Company (NOC) in Kirkuk for their cooperation in releasing the data used in this study.

Reference

[1] T. Buday, The Regional Geology of Iraq Vol.1, Baghdad: GEUSURV, 1980.

[2] J. A. Al-Sakini, "Summary of petroleum geology of Iraq and the Middle East," Northern Oil Company Press, Kirkuk, 1992.

[3] [3] L. R. Litsey, K. M. Al-Hinai, N. B. DisMukes and W. L. MacBride, "Shu’aiba Reservoir Geological Study, Yibal Field, Oman," Journal of Petroleum Geology, vol. 38, no. 6, pp. 651-661, 1986.

[4] A. S. Al-Sharhan, "Depositional Environment, Reservoir units Evolution, and Hydrocarbon Habitat of Shu'aiba Formation, Lower Cretaceous, Abu Dhabi, United Arab Emirates," AAPG Bulletin, vol. 69, no. 6, pp. 899-912, 1985.

[5] A. AI-Siddiqi and R. A.Dawe, "A Review of Petroleum Engineering Aspects of Qatar's Oil and Gas," Engineering Journal of the University of Qatar, vol. 11, pp. 11- 45, 1998.

[6] M. Abuali, "The Paleozoic and Mesozoic Petroleum Systems of Saudi Arabia," in Geo Convention Conference, Calgary, Canada, 2018.

[7] N. M. Al-Ghamdi, Facies, Sequence Framework, and Evolution of Rudist Buildups, Shu'aiba Formation, Saudi Arabia, Virginia: MSc Thesis, Virginia Polytechnic Institute and State University, 2008.

[8] Z. A. Al-Shawi, M. M. Mahdi and A. H. Mohammed, "New records of planktonic foraminifera in the Shuaiba Formation (Aptian Age), Mesopotamian plain, South of Iraq," Iraqi Journal of Science, vol. 60, no. 6, pp. 1322-1335, 2019.

[9] A. S. Al-Banna and M. A. Al-Khafaji, "Well Log Analysis of Nahr Umr, Shuaiba and Zubair Formations in EB-4 well of East Baghdad Oil Field, Iraq, using Rock Physics Templates (RPTs)," Iraqi Journal of Science, vol. 62, no. 3, pp. 927-940, 2021.

[10] R.C.Van. Bellen, H.V. Dunnington, R. Wetzel and D. Morton, Lexique Stratigraphique, International. Asie, Iraq, Paris, France: CNRS, 1959.

[11] S.Z. Jassim and J.C. Goff, Geology of Iraq, Brno: Dolin, Prague and Moravian Museum, 2006.

[12] P.R. Sharland, R. Archer, D.M. Casey, R.B. Davies, S.H. Hall, A.P. Heward, A.D. Horbury and M.D. Simmons, "The Chrono Sequence Stratigraphy of the Arabian Plate," Geoarabia, vol. Special Publication, no. 2, 2001.

[13] A.A.M. Aqrawi, A.D. Horbury, J.C. Guff, and F.N. Sadooni, The Petroleum Geology of Iraq, Beaconsfield, UK: Scientific Press Ltd., 2010.

[14] V. Ditmar and Iraqi-Soviet Team, "Geological conditions and hydrocarbon prospects of the Republic of Iraq (Northern and Central parts)," INOC, Baghdad, Iraq, 1971.

[15] NOC, "A geological study of the Cretaceous reservoirs in Bai-Hassan Field," Northern Oil Company, Kirkuk, Iraq, unpublished internal report 1992.

[16] S. Al-Shdidi, G. Thomas and J. Deluad, "Sedimentology, Diagenesis and Oil Habitat of Lower Cretaceous Group, Northern Iraq," AAPG, vol. 79, no. 5, pp. 63-779, 1995.

[17] M. A. Al-Eisa, Stratigraphy of Early Cretaceous of Subsurface Sections from Middle Iraq, Mosul, Iraq: PhD Dissertation, University of Mosul, 1997.

[18] B. M. Ameen, Sedimentology and Lithostratigraphy of Qamchuqa Formation from Kurdistan Region, NE-Iraq, Sulaimani, Iraq: PhD Dissertation, University of Sulaimani, 2007.

[19] Q. M. Sadeq, Q. Dezday, S. K. Bhattacharya and W. I. B. Wan Yusoff, "Permeability Estimation of Fractured and Vuggy Carbonate Reservoir by Permeability Multiplier Method in Bai Hassan Oil Field Northern Iraq," Petroleum and Environmental Biotechnology, vol. 6, no. 4, 2015.

[20] F. Qader and B. Al-Qayim, "Petrophysical and sedimentological characterization of the Aptian Shu'aiba (Lower Qamchuqa) Formation, Khabaz oil Field, Northern Iraq," Journal of Petroleum Geology, vol. 39, no. 4, pp. 375-392, 2016.

[21] F. N. Al-Sadooni, The sedimentology and petroleum prospects of the Qamchuqa Group from Kirkuk, Bai Hassan and Jambur Oilfields, Bristle, UK: PhD Dissertation, University of Bristle, 1978.

[22] A. Bennacef, Depositional cycle, Cretaceous of the west Tigris faulted area, seismic stratigraphy and correlation of wells, Paris, France: Total CFP, 1989.

[23] M. Moulade, B. Peybemes, J. Rey and P. Saint-Marc, "Biostratigraphic interest and paleobiogeographic distribution of early and middle cretaceous Mesogean Orbitolina (foraminiferidal)," Jour. of foraminiferal research, vol. 15, no. 3, pp. 149-158, 1985.

[24] OEC, "The annual report about the reservoirs for the year 1993," Iraqi Oil Exploration Company, Baghdad, Iraq, 1994.

[25] J. K. Pitman, D. Steinshouer and M. D. Lewan, "Petroleum generation and migration in the Mesopotamian basin and Zagros fold belt of Iraq, results from a basin-modeling study," GeoArabia, vol. 9, no. 4, pp. 41-72, 2004.

[26] R. J. Dunham, "Classification of carbonate rocks according to depositional texture," in Classification of carbonate rocks: In W. E. Ham (ed.), USA, American Association of Petroleum Geologists Memoir, 1962, pp. 108-121.
[27] E. Flugel, Microfacies of Carbonate Rocks, Analysis, Interpretation and Application, New York, USA: Springer, 2004.
[28] M. Ghorab, A. M. Ramadan and A. Z. Nouh, "The Relation between the Shale Origin (Source or Non-Source) and its Type for Abu Roash formation at Wadi El-Natrun Area, South of Western Desert, Egypt," Australian Journal of Basic and Applied Sciences, vol. 2, no. 3, pp. 360-371, 2008.
[29] Schlumberger, Log Interpretation / Charts, Houston, USA: Schlumberger Wireline and Testing, 1997.
[30] G. Asquith and D. Krygowski, Basic Well Log Analysis (2nd Edition), Methods in Exploration No.16, Tulsa, Oklahoma, USA: AAPG, 2004.
[31] S. Mohaghehet, B. Balan and S. Ameri, "Permeability determination from well log data," SPE, vol. 12, no. 3, pp. 170-174, 1997.
[32] R. S. Buckles, "Correlating and averaging connate water saturation data," Journal of Canadian Petroleum Technology, vol. 9, no. 1, pp. 42-52, 1965.
[33] A. Humbolt, Genetic pore typing as a means of characterizing reservoir flow units. Sanandres, Sunflower field, Terry County, Texas, Texas: MSc Thesis, A&M University, USA, 2006.
[34] J. O. Amaefule, M. Altunbay, D. Tiab, D. G. Kersey and D. K. Keelan, "Enhanced Reservoir Description: Using core and log data to identify hydraulic (flow) Units and predict permeability in Uncored Intervals/Wells," in 68th Annual Tech. Conf. Paper SPE 26435, Houston, TX, USA, 1993.
[35] W. J. Teh, G. P. Willhite, J. H. Doveton and J. S. Tsau, Improved Predictions of Porosity from Micro resistivity Logs in a Mature Field through Incorporation of Pore Typing, Columbus, Ohio, USA: Paper presented in SPE meeting, paper no. (SPE-149506-MS), 2011, pp. 149-506.
[36] C. L. Hear, W. J. Ebanks, R. S. Tye and V. Ranganatha, "Geological Factors Influencing Reservoir Performance of the Hartzog Draw Field, Wyoming," J. of Petrol. Tech, vol. 30, no. 8, pp. 1335-1344, 1984.
[37] H. A. Baker, S. N. AL-Jawad and Z. I. Murtadha, "Permeability Prediction in Carbonate Reservoir Rock Using FZI," Iraqi Journal of Chemical and Petroleum Engineering, vol. 14, no. 3, pp. 49-54, 2013.
[38] Schlumberger, Log Interpretation, Vol. I Principles, New York, USA: Schlumberger Limited, 1972.
[39] G. B. Asquith, Handbook of log evaluation techniques for carbonate Reservoirs, Tulsa, Oklahoma USA: AAPG, 1985.
[40] E. Egbele, I. Ezuka and M. Onyekonwu, "Net-To-Gross Ratios: Implications in Integrated Reservoir Management Studies.," in Nigeria Annual International Conference and Exhibition. Society of Petroleum Engineers, Nigeria, 2005.
[41] E. J. Peters, Advanced Petrophysics, Texas, USA: University of Texas, 2001.
[42] A. Law, J. Megson and M. Pye, "Low Permeability Reservoirs: Introduction," Petroleum Geoscience, vol. 7, no. 1, p. 2, 2001.
[43] D. Tiab and E. C. Donaldson, Petrophysics-Theory and Practice of Measuring Reservoir Rock and Fluid Transport Properties (2nd Edition), Boston, USA: Gulf Publishing Co., 2004.
[44] T. Darling, Well logging and Formation Evaluation, Amsterdam, Netherland: Elsevier, 2005.
[45] J. Parnell, C. W. Taylor, S. Thackrey, R. Gordon, S. Osinski and L. Lee, "Permeability data for impact breccias imply focused hydrothermal fluid flow," Journal of Geochemical Exploration, vol. 106, no. 1-3, pp. 171-175, 2010.